

Frame Synchronization for Variable-Length Packets

Watcharapan Suwansantisuk, *Student Member, IEEE*, Marco Chiani, *Senior Member, IEEE*, and Moe Z. Win, *Fellow, IEEE*

Abstract—A cognitive radio can sense its environment and adapt some of its features, such as carrier frequency, transmission bandwidth, transmission power, and modulation, thus allowing dynamic reuse of the available spectrum. Due to their high degree of adaptability to environmental variations, cognitive radios are expected to utilize packet-based transmission with variable-length frames. Packet-based transmission requires the receiver to perform frame synchronization, an important enabling step that allows adaptation in cognitive radios. However, proper metrics to characterize the performance of frame synchronization for transmission of variable-length frames are currently unavailable. To address this issue, we put forth two performance metrics, namely the expected duration to complete frame synchronization and the probability of correct acquisition within a given duration. We then develop analytical expressions for these important metrics. This paper advances our understanding of frame synchronization for the continuous transmission of variable-length frames and for bursty transmission.

Index Terms—Frame synchronization, cognitive radios, hypothesis testing, detection, synchronization patterns.

I. INTRODUCTION

THE COGNITIVE radio concept aims at providing a more efficient and flexible usage of the radio spectrum [1]–[5]. It has been observed that, most of the time, some frequency bands are largely unoccupied or partially occupied and that the remaining frequency bands are heavily used. The frequency bands that are underutilized are commonly referred to as *the spectrum holes* [2]–[5]. In order to improve spectrum utilization, these spectrum holes could be utilized by secondary users at the appropriate location and time.

Cognitive radio permits, in principle, a more efficient use of the radio spectrum. The basic idea is that a cognitive radio terminal can sense its environment and then adapt some of its features to allow the dynamic reuse of the available spectrum. This could lead to a multidimensional reuse of the spectrum in space and time, overcoming spectrum scarcity, which has been an obstacle for broadband wireless communication development.

Manuscript submitted March, 2007; revised September, 2007. This research was supported, in part, by the Office of Naval Research Young Investigator Award N00014-03-1-0489, the National Science Foundation under Grants ANI-0335256 and ECS-0636519, DoCoMo USA Labs, the Charles Stark Draper Laboratory Reduced Complexity UWB Communication Techniques Program, the Institute of Advanced Study Natural Science & Technology Fellowship, the University of Bologna Grant “Internazionalizzazione,” and the European Commission under project FP6 IST-001812 “PHOENIX.”

W. Suwansantisuk and M. Z. Win are with the Laboratory for Information and Decision Systems (LIDS), Massachusetts Institute of Technology, Room 32-D666, 77 Massachusetts Avenue, Cambridge, MA 02139 USA (e-mail: wsk@mit.edu, moewin@mit.edu).

M. Chiani is with DEIS, University of Bologna, V.le Risorgimento 2, 40136 Bologna, ITALY (e-mail: mchiani@deis.unibo.it).

Digital Object Identifier 10.1109/JSAC.2008.080106.

One of the key issues is in the inherent adaptability that cognitive radio terminals must have. In particular, adaptation to environmental changes (in the available bandwidth, interference level, fading, path-loss, etc.) includes adaptive source coding, channel coding, and modulation. When designing adaptive source/channel coding and modulation for cognitive radio, one must account for the fact that some of the most important source encoders, such as MPEG4 and H264 for multimedia, produce frames of variable lengths, depending on the scene [6], [7]. Due to the high degree of adaptability to environmental variations and due to the multimedia nature of the sources,¹ it is envisioned that most cognitive radio systems will use packet-based transmission, where the frames are not necessarily of constant lengths. In this paper we discuss unique challenges associated with frame synchronization problem in cognitive radio.

Digital transmission among cognitive radios requires a receiver to regulate its clock in synchronism with the transmitter clock. Clock synchronism is achieved at the waveform level (by an acquisition unit and a phase-locked loop), at the symbol level (by a bit synchronizer), and then at the frame level (by a frame synchronizer) [10] [11, pp. 7–8]. Issues related to waveform and bit synchronization are relatively well understood [12]–[29] but frame synchronization, especially for cognitive radios, is largely an unexplored area.²

Frame synchronization involves the following steps. In the first step, the transmitter injects a fixed-length symbol pattern, called a marker, into the beginning of each frame³ to form a marker and frame pair, which is known as a packet (Fig. 1).⁴ Packets are then converted from symbols into a waveform and transmitted through the channel. The receiver detects the arrival of packets by searching for the marker, removes the markers from the data stream, and recovers the transmitted messages. Marker detection is the most important step for frame synchronization.

The division of symbols into frames may seem burdensome for the network, but it serves many purposes. Framing ensures that individual frames can be transmitted independently without requiring scheduling overhead. The ability to transmit individual frames independently implies that the spectrum can be utilized intermittently according to its availability, resulting in efficient spectrum utilization. In the streaming

¹In multimedia communication systems, it has been shown that performance improvements can be achieved by moving from separate source and channel codes to a joint source-channel code (JSCC) design [8], [9].

²According to our terminology, [26]–[29] are regarded as bit synchronization.

³Before injecting markers, the transmitter modifies the sequence of data symbols, if necessary, to ensure that the data symbols differ from the marker symbols.

⁴The marker is also known as the receiver.

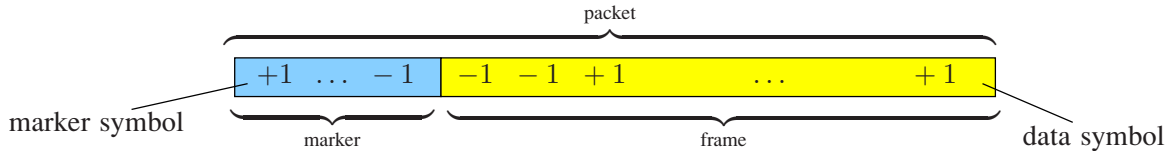


Fig. 1. A packet consists of two parts: a marker and a frame. The marker indicates the start of a frame, while the frame contains transmitted messages and other relevant information, such as the frame lengths and the symbol pattern for channel estimation.

of multimedia data (such as MPEG-4 video [30]), framing ensures that errors within one frame do not propagate to adjacent frames [6], [7]. In a network that employs legacy transmission systems, such as asynchronous transfer mode (ATM) technology [31], framing ensures that frames have a length that can be handled by the underlying network infrastructure. These examples show that frame synchronization is important for various applications including cognitive radio.

Several approaches can be employed to achieve frame synchronization. One approach, referred to as a continuous transmission of packets, is to reserve the communication link between the transmitter and receiver over the entire time of communication. Frames for continuous transmission may have a fixed length [32]–[35] (such as those in ATM networks) or variable lengths [36]–[38] (such as those in MPEG-4 video streaming). In both cases, the transmitter sends a special character, known as an idle fill character, when it has no immediate packet to transmit (Fig. 2). The idle fill characters serve the purpose of keeping the transmitter and receiver synchronized. The use of idle fill characters is possible since the entire link is allocated to the transmitter and receiver during continuous transmission.

On the other hand, the link may not be allocated to the transmitter and receiver during the communications. This approach, referred to as bursty packet transmission, arises in practice, for example, in an 802.11 network and in the Internet. For cognitive radios, bursty transmission provides benefits that include a low transmission overhead and efficient spectrum utilization. The drawback of bursty transmission is that transmission delay is difficult to control, which could be problematic for transmission of time-critical information. Bursty transmission uses variable frame-lengths, and, unlike continuous transmission, idle fill characters cannot be used to maintain synchronization between the transmitter and receiver (see Fig. 3). As a result, marker detection strategies for continuous and bursty transmission are different.

Performance of frame synchronization can be improved by two broad design approaches. The first approach improves the performance through the design of a marker with good synchronization properties [39]–[43]. The second approach improves the performance through the design of optimal or near-optimal marker-detection strategies [34]–[38], [44]. The problem of marker design, valid for both continuous and bursty transmission schemes, has been explored [39]–[43]. In contrast, the problem of optimal marker-detection strategies is only well-understood for the transmission of fixed-length frames. This paper focuses on issues related to transmission of variable-length frames.

Transmission of variable-length frames, continuous or bursty, presents challenges from a mathematical point of view.

Variable-length frames imply that mathematical models for a fixed-length frames are no longer valid. As a result, one needs to develop a suitable mathematical framework for understanding frame synchronization of variable-length frames. A commonly-used metric to characterize the performance of marker detection for frame synchronization is the receiver operating characteristic (ROC). However, this performance metric neither captures the frame loss rate in the case of bursty transmission nor characterizes the synchronization time in the case of variable-length frame transmission. More meaningful performance metrics in the case of variable length frames are (a) the expected duration to complete frame synchronization and (b) the probability of completing frame synchronization within a given duration. Despite their usefulness, closed-form expressions for such metrics are currently unavailable. As a result, these metrics are usually obtained via Monte Carlo simulation [45]–[47].

In this paper we investigate frame synchronization for transmission of variable-length frames.⁵ The main contributions of the paper are as follows:

- We develop a mathematical framework and methodology for the design and analysis of frame synchronization systems that are applicable to a broad class of scenarios, encompassing various receiver architectures, fading conditions, and operating environments; and
- We put forth and analyze two important performance metrics, namely the expected duration to complete frame synchronization and the probability of completing frame synchronization within a given duration.

The results will advance the fundamental understanding of frame synchronization for the continuous transmission of variable-length frames and for bursty transmission of frames, which are the two important transmission modes foreseen for cognitive radios.

The remaining sections are organized as follows. Sec. II presents the system model. Sec. III derives the expected duration to complete frame synchronization and the probability of completing frame synchronization within a given duration. Sec. IV derives the probability that a correct acquisition occurs within a given duration. Sec. V outlines a numerical approach to obtaining these performance metrics. Sec. VI assesses the computation time required to evaluate the performance metrics. Sec. VII provides numerical results. Sec. VIII concludes the paper and summarizes important findings.

II. SYSTEM MODEL

In this section we start by describing aspects of the transmitter and receiver which are relevant to the frame synchro-

⁵In the following, we will use the phrase “frame synchronization” to refer to frame synchronization of variable-length frame transmission, continuous or bursty.

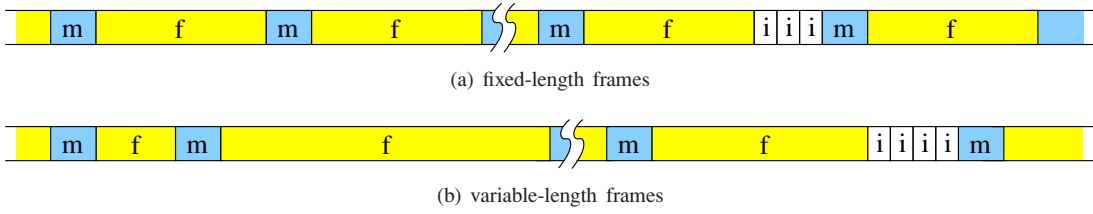


Fig. 2. Idle fill characters keep the transmitter and receiver synchronized for the continuous transmission. Here, region “m” indicates a marker, “f” indicates a frame, and “i” indicates an idle fill character.



Fig. 3. The use of idle fill characters is not allowed in bursty transmission. Hence, the time between two packets is silent.

nization problem. We then present the marker acquisition procedure and introduce the concept of arrival process.

The transmitter delimits a long sequence of data to generate frames of variable lengths. Frame lengths or the number of data symbols per frame, $\{L_i^d : i \geq 1\}$, can be modeled as independent and identically distributed (i.i.d.) random variables. The transmitter injects a marker, $(c_1, c_2, \dots, c_{\ell_{\max}^m})$, of fixed length, $\ell_{\max}^m \geq 2$ symbols, before each frame to form a packet. A modulator then generates a waveform from a sequence of data and marker symbols to be transmitted through the channel.

Adjacent packets are separated by an interval of length L_i^s , where $\{L_i^s : i \geq 1\}$ are i.i.d. and independent of L_i^d (see Fig. 4). Each L_i^s corresponds to the length of the idle fill characters in the case of continuous transmission or the length of silence in the case of bursty transmission. The waveform representing the packets and separation intervals is corrupted by noise and fading. The corrupted waveform becomes an input to the receiver.

Upon receiving an input waveform, the receiver generates a sequence of soft decision variables, $\{X_j : j \geq 1\}$, which forms the input for the frame synchronizer. Variable X_j represents a corrupted marker symbol, a corrupted data symbol, or a corrupted symbol corresponding to the silent transmission. The frame synchronizer is said to acquire a marker at an index k if it decides, either correctly or incorrectly, that the soft-decision variable X_k corresponds to the first symbol of the marker.

To acquire a marker, the frame synchronizer forms a real-valued decision variable,⁶

$$V_j = g(X_{j:j+\ell_{\max}^m-1}),$$

for each symbol time, $j \geq 1$, where $x_{j:k}$ denotes a vector $[x_j x_{j+1} \dots x_k]$ for $j \leq k$. If the decision variable V_j belongs to a predetermined set, \mathcal{R} , of real numbers, the frame synchronizer acquires a marker at index j .⁷ Otherwise, the frame synchronizer tests the next decision variable, V_{j+1} .

⁶Recall that the length of markers is ℓ_{\max}^m . We consider the case, in which only ℓ_{\max}^m consecutive X_j 's are required in forming the decision variable.

⁷For example, the set \mathcal{R} can be $[\eta, \infty)$ for the case that $L_i^s = 0$ and for binary antipodal modulation, where η is known as a threshold.

Examples of g are given by

$$g_1(X_{j:j+\ell_{\max}^m-1}) = \sum_{k=1}^{\ell_{\max}^m} c_k X_{j+k-1}, \quad (1)$$

$$g_2(X_{j:j+\ell_{\max}^m-1}) = \sum_{k=1}^{\ell_{\max}^m} [c_k X_{j+k-1} - |X_{j+k-1}|], \quad (2)$$

for antipodal marker symbols [37], [38]. Note that random variables $\{V_j\}$ are not mutually independent. In fact, this property makes the exact derivations of the performance metrics challenging.

In this setting, the classical method [17] for analyzing the problem of synchronizing spread-spectrum waveforms does not apply since it assumes a constant frame length (which equals the spreading sequence period). In contrast, the spacing, $L_i^d + L_i^s + \ell_{\max}^m$, between the adjacent markers in frame synchronization varies from one packet to another. Here, we propose to analyze the frame synchronization problem by employing mathematical tools developed for studying the arrival processes.

A systematic approach to obtain performance metrics for frame synchronization involves the use of an arrival process, $\{J_i\}$, in which $1 \leq J_1 < J_2 < J_3 < \dots$ denote arrival times of markers. An arrival is said to occur at time $j \in \mathbb{Z}_+$, if the first symbol of the marker begins at index j (and hence the decision variable V_j belongs to \mathcal{R} under an ideal case).⁸ We refer to a sequence of discrete time $\{j : J_i < j \leq J_{i+1}\}$ as a marker spacing span (MSS), with the convention that $J_0 < 1$. It will be apparent that the time until the first arrival, J_1 , and interarrival times, $T_i \triangleq J_{i+1} - J_i = L_i^d + L_i^s + \ell_{\max}^m$, play an important role in the analysis.⁹

We consider a time invariance property for the decision variables. In particular, the probabilities

$$\mathbb{P}\{V_{J_i+1:J_{i+1}} \in \mathcal{R}^c \mid V_{J_i-\ell_{\max}^m+2:J_i} \in \mathcal{R}^c\}$$

are identical for any i , and so are

$$\mathbb{P}\{V_{J_i+1:J_{i+1}-1} \in \mathcal{R}^c, V_{J_i+1} \in \mathcal{R} \mid V_{J_i-\ell_{\max}^m+2:J_i} \in \mathcal{R}^c\}.$$

Intuitively, the time invariance property states that statistical properties of the decision variables within an MSS do not depend on the choice of MSS. Time invariance property is

⁸The symbol \mathbb{Z}_+ denotes the set of all positive integers.

⁹In general, the time until the first arrival J_1 and interarrival time T_i have different distributions.

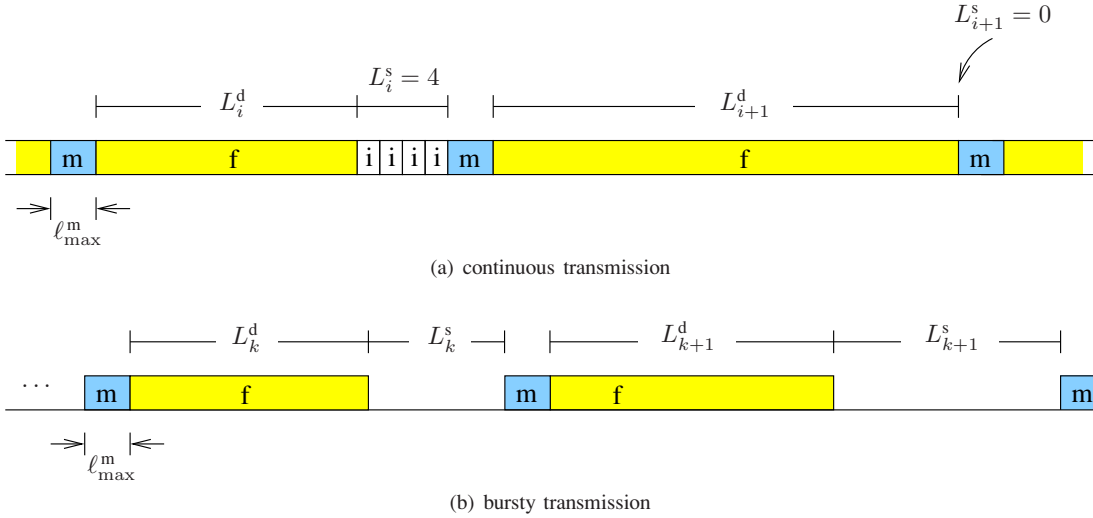


Fig. 4. Two adjacent packets are separated by an interval, during which the transmitter has no data to send.

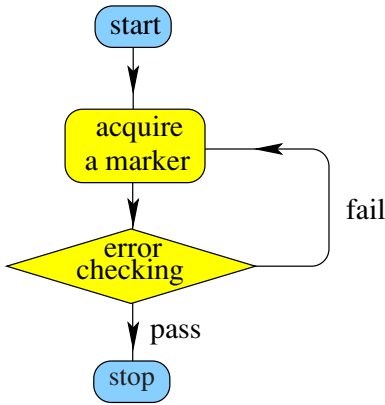


Fig. 5. The diagram represents the frame synchronization process, which terminates after the correct acquisition of a marker.

valid when the probability of transmitting a given symbol, the channel statistics, and the decision rule do not change during frame synchronization.

III. EXPECTED NUMBER OF MSSS REQUIRED FOR A CORRECT ACQUISITION

The frame-synchronization process ends when the receiver acquires a correct marker. When an incorrect marker acquisition occurs, we assume that data symbols in the frame will be recognized as incorrect, for example by means of verifying the frame structure or by means of cyclic redundancy check (CRC). After an incorrect acquisition is detected, the search for a marker starts all over again. These procedures are represented by the diagram in Fig. 5.

To measure the amount of time required to synchronize correctly, we count the number of MSSs that are needed for a correct acquisition. Such a number is denoted by a random sum, M , which is equal to

$$M = \sum_{i=1}^K M_i, \quad (3)$$

where $K \geq 1$ is a random variable representing the number of attempts until frame synchronization ends and $M_i \geq 1$ are

random variables representing the required number of MSSs for attempt i . The expected number of MSSs required for a correct acquisition, $\mathbb{E}\{M\}$, is a suitable metric for frame synchronization.

We consider $\{M_i\}$ to be i.i.d. and K to have a geometric distribution with probability of success p_{cAcq} , where p_{cAcq} denotes the probability that a marker acquisition is correct. This can be justified as follows. Typically, an error-checking process lasts on the order of the frame length. Hence, different synchronization attempts examine different portions of the MSSs, implying that $\{M_i\}$ are independent. Furthermore, it is reasonable to model a time instant at which an incorrect acquisition occurs as a random variable. Therefore the arrival processes observed during different attempts are identically distributed, implying that $\{M_i\}$ are identically distributed. Therefore, $\{M_i\}$ are i.i.d., and K has a geometric distribution with probability of success p_{cAcq} .

Using the above model, we show in Appendix A that¹⁰

$$\mathbb{E}\{M\} = \mathbb{E}\{M_1\} \mathbb{E}\{K\}. \quad (4)$$

Substituting $\mathbb{E}\{K\} = 1/p_{cAcq}$ gives

$$\mathbb{E}\{M\} = \mathbb{E}\{M_1\} / p_{cAcq}. \quad (5)$$

Defining¹¹

$$p_{\text{nal}} \triangleq \mathbb{P}\{V_1: J_1 \in \mathcal{R}^c\}, \quad (6a)$$

$$p_{\text{det}} \triangleq \mathbb{P}\{V_1: J_1 - 1 \in \mathcal{R}^c, V_{J_1} \in \mathcal{R}\}, \quad (6b)$$

$$p_{\text{nal-nal}} \triangleq \mathbb{P}\{V_1: J_2 \in \mathcal{R}^c\}, \quad (6c)$$

$$p_{\text{nal-det}} \triangleq \mathbb{P}\{V_1: J_2 - 1 \in \mathcal{R}^c, V_{J_2} \in \mathcal{R}\}, \quad (6d)$$

$$c_{\text{nal}} \triangleq \mathbb{P}\{V_{J_2+1}: J_3 \in \mathcal{R}^c \mid V_{J_2-l_{\text{max}}+2}: J_2 \in \mathcal{R}^c\}, \quad (6e)$$

¹⁰Note that the equation is not a direct application of the iterated law of expectation [48, p. 323] since we do not require K and M_1 to be independent.

¹¹When $J_1 = 1$, we define $p_{\text{det}} \triangleq \mathbb{P}\{V_{J_1} \in \mathcal{R}\}$. The subscript “det” stands for “detection,” which refers to a detection of the marker. The subscript “nal” stands for “no alarm,” which refers to the situation that decision variables under consideration belong to \mathcal{R}^c .

and

$$c_{\text{det}} \triangleq \mathbb{P}\{V_{J_2+1}: J_3-1 \in \mathcal{R}^c, V_{J_3} \in \mathcal{R} | \\ V_{J_2-\ell_{\text{max}}^m+2}: J_2 \in \mathcal{R}^c\}, \quad (6f)$$

we show in Appendix B that

$$p_{\text{cAcq}} = \begin{cases} p_{\text{det}} + p_{\text{nal-det}}, & \text{if } c_{\text{nal}} = 1; \\ p_{\text{det}} + p_{\text{nal-det}} + \frac{p_{\text{nal-nal}}c_{\text{det}}}{1-c_{\text{nal}}}, & \text{if } 0 \leq c_{\text{nal}} < 1, \end{cases} \quad (7)$$

and, in Appendix C that

$$\mathbb{E}\{M_1\} = \begin{cases} 1 + p_{\text{nal}} + \frac{p_{\text{nal-nal}}}{1-c_{\text{nal}}}, & \text{if } 0 \leq c_{\text{nal}} < 1; \\ 1 + p_{\text{nal}}, & \text{if } c_{\text{nal}} = 1 \text{ and } p_{\text{nal-nal}} = 0; \\ \infty, & \text{if } c_{\text{nal}} = 1 \text{ and } 0 < p_{\text{nal-nal}} \leq 1. \end{cases} \quad (8)$$

For convenience, the probabilities in (6) will be referred to as the transition probabilities. In the next section, we will derive another performance metric, which is suitable for bursty transmission.

IV. PROBABILITY OF CORRECTION ACQUISITION WITHIN A GIVEN DURATION

The performance metric introduced in the previous section is suitable for transmission systems without delay constraints. For systems with delay constraints, e.g., bursty transmission systems, an appropriate performance metric is the probability of correct acquisition within a given duration.

The probability of correct acquisition within m MSSs is equal to $\mathbb{P}\{M \leq m\}$, where the random variable M is defined in Sec. III. Then,

$$\mathbb{P}\{M \leq m\} = \sum_{k=1}^{\infty} \mathbb{P}\{M_1 + M_2 + \dots + M_k \leq m | K = k\} \mathbb{P}\{K = k\} \\ = \sum_{k=1}^m \underbrace{\mathbb{P}\{M_1 + M_2 + \dots + M_k \leq m\}}_{\triangleq \gamma(k,m)} (1 - p_{\text{cAcq}})^{k-1} p_{\text{cAcq}},$$

where $(1 - p_{\text{cAcq}})^0 \triangleq 1$. The upper limit of the summation becomes finite since

$$\mathbb{P}\{M_1 + M_2 + \dots + M_k \leq m\} = 0$$

for $m < k$, owing to the fact that $M_i \geq 1$. The function $\gamma(k, m)$ for $1 \leq k \leq m$ is given by a recursive formula (see Appendix D)

$$\gamma(1, m) = 1 - \mathbb{P}\{M_1 \geq m + 1\}, \quad \text{for } 1 \leq m \quad (9a)$$

$$\gamma(k+1, m) = \sum_{n=1}^{m-k} \gamma(k, m-n) \mathbb{P}\{M_1 = n\}, \\ \text{for } 0 < k < m, \quad (9b)$$

where

$$\mathbb{P}\{M_1 = n\} = \mathbb{P}\{M_1 \geq n\} - \mathbb{P}\{M_1 \geq n + 1\}, \\ \text{for } n = 1, 2, 3, \dots,$$

and according to Appendix C,

$$\mathbb{P}\{M_1 \geq n\} = \begin{cases} 1, & \text{for } n = 1; \\ p_{\text{nal}}, & \text{for } n = 2; \\ p_{\text{nal-nal}}, & \text{for } n = 3; \\ p_{\text{nal-nal}}(c_{\text{nal}})^{n-3}, & \text{for } n \geq 4. \end{cases}$$

This completes the derivation of the second performance metric.

V. DERIVATION FOR THE TRANSITION PROBABILITIES

To obtain the performance metrics derived in previous two sections, we need to evaluate the transition probabilities given in (6). This section outlines approaches to derive these transition probabilities.

A. Derivation for p_{nal}

Let ℓ_{max}^d denote the maximum frame length and ℓ_{max}^s denote the maximum length of silent transmission: $L_1^d \leq \ell_{\text{max}}^d$ and $L_1^s \leq \ell_{\text{max}}^s$. Let L_0^d and L_0^s denote the length of the frame and the length of silent transmission, respectively, of the MSS that contains the first observed symbol. We write

$$p_{\text{nal}} = \mathbb{P}\{V_1: J_1 \in \mathcal{R}^c\} \\ = \sum_{\ell_0^d=1}^{\ell_{\text{max}}^d} \sum_{\ell_0^s=0}^{\ell_{\text{max}}^s} \sum_{j_1=1}^{\ell_0^d+\ell_0^s+\ell_{\text{max}}^m} \mathbb{P}\{V_1: J_1 \in \mathcal{R}^c | \\ J_1 = j_1, L_0^d = \ell_0^d, L_0^s = \ell_0^s\} \\ \times \mathbb{P}\{J_1 = j_1 | L_0^d = \ell_0^d, L_0^s = \ell_0^s\} \\ \times \mathbb{P}\{L_0^d = \ell_0^d\} \mathbb{P}\{L_0^s = \ell_0^s\},$$

where each probability term inside the summation can be obtained as follows.

The probabilities $\mathbb{P}\{L_0^d = \ell_0^d\}$ and $\mathbb{P}\{L_0^s = \ell_0^s\}$ are given by (see Appendix E)

$$\mathbb{P}\{L_0^d = \ell_0^d\} = \left(\frac{\ell_0^d + \mathbb{E}\{L_1^s\} + \ell_{\text{max}}^m}{\mathbb{E}\{L_1^d\} + \mathbb{E}\{L_1^s\} + \ell_{\text{max}}^m} \right) \mathbb{P}\{L_1^d = \ell_0^d\} \quad (10a)$$

$$\mathbb{P}\{L_0^s = \ell_0^s\} = \left(\frac{\ell_0^s + \mathbb{E}\{L_1^d\} + \ell_{\text{max}}^m}{\mathbb{E}\{L_1^d\} + \mathbb{E}\{L_1^s\} + \ell_{\text{max}}^m} \right) \mathbb{P}\{L_1^s = \ell_0^s\}. \quad (10b)$$

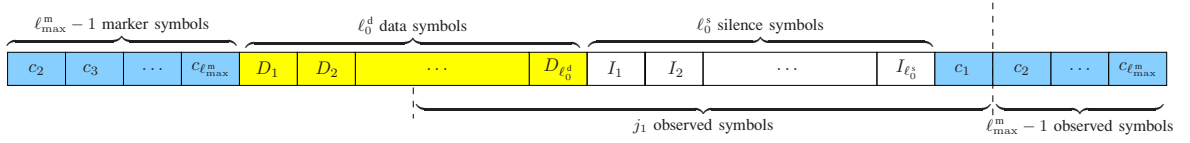
On the other hand, the conditional probability $\mathbb{P}\{J_1 = j_1 | L_0^d = \ell_0^d, L_0^s = \ell_0^s\}$ is uniform over the length of the MSS, since the first observed symbol can be anywhere in the MSS:

$$\mathbb{P}\{J_1 = j_1 | L_0^d = \ell_0^d, L_0^s = \ell_0^s\} \\ = \begin{cases} \frac{1}{\ell_0^d + \ell_0^s + \ell_{\text{max}}^m}, & \text{for } 1 \leq j_1 \leq \ell_0^d + \ell_0^s + \ell_{\text{max}}^m; \\ 0, & \text{otherwise.} \end{cases}$$

The conditional probability

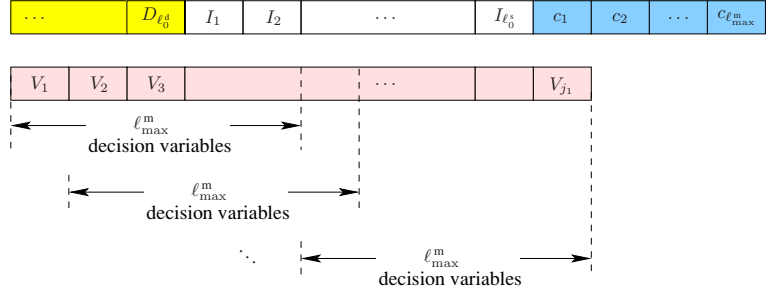
$$\mathbb{P}\{V_1: J_1 \in \mathcal{R}^c | J_1 = j_1, L_0^d = \ell_0^d, L_0^s = \ell_0^s\}$$

for $1 \leq j_1 \leq \ell_{\text{max}}^m$ can be obtained by integrating the conditional joint probability density function (pdf) over the

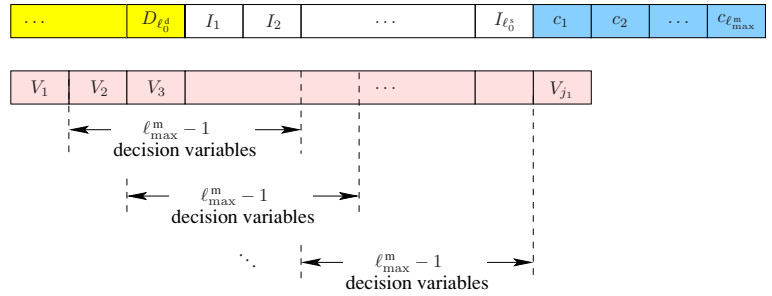


observation begins here

(a) Sequence of symbols satisfying the condition $\{J_1 = j_1, L_0^d = \ell_0^d, L_0^s = \ell_0^s\}$



(b) Blocks of length ℓ_{\max}^m , each of which corresponds to a different ℓ_{\max}^m -joint probability term in the numerator



(c) Blocks of length $\ell_{\max}^m - 1$, each of which corresponds to a different $(\ell_{\max}^m - 1)$ -joint probability term in the denominator

Fig. 6. Pictorial representation of the MSS helps to aid the interpretation of equation (11).

region $(\mathcal{R}^c)^{j_1}$.¹² For $j_1 \geq \ell_{\max}^m + 1$, we obtain the conditional probability through the expansion (11) at the bottom of the page.

¹²The symbol \mathcal{A}^{j_1} for a set \mathcal{A} refers to the Cartesian product $\mathcal{A} \times \mathcal{A} \times \dots \times \mathcal{A}$, where \mathcal{A} appears j_1 times.

Equation (11) can be interpreted with the help of Fig. 6 as follows. The condition $\{J_1 = j_1, L_0^d = \ell_0^d, L_0^s = \ell_0^s\}$ indicates that the observed symbols are the last j_1 symbols of an MSS with length $\ell_0^d + \ell_0^s + \ell_{\max}^m$, followed by $\ell_{\max}^m - 1$ marker symbols (see Fig. 6a). These observed symbols generate a total of j_1 decision variables. Each of the $j_1 - \ell_{\max}^m + 1$ terms

$$\begin{aligned}
 & \mathbb{P}\{V_{1:j_1} \in \mathcal{R}^c \mid J_1 = j_1, L_0^d = \ell_0^d, L_0^s = \ell_0^s\} \\
 &= \mathbb{P}\{V_{1:\ell_{\max}^m} \in \mathcal{R}^c \mid J_1 = j_1, L_0^d = \ell_0^d, L_0^s = \ell_0^s\} \prod_{k=\ell_{\max}^m+1}^{j_1} \mathbb{P}\{V_k \in \mathcal{R}^c \mid V_{k-\ell_{\max}^m+1:k-1} \in \mathcal{R}^c, J_1 = j_1, L_0^d = \ell_0^d, L_0^s = \ell_0^s\} \\
 &= \mathbb{P}\{V_{1:\ell_{\max}^m} \in \mathcal{R}^c \mid J_1 = j_1, L_0^d = \ell_0^d, L_0^s = \ell_0^s\} \prod_{k=\ell_{\max}^m+1}^{j_1} \frac{\mathbb{P}\{V_{k-\ell_{\max}^m+1:k} \in \mathcal{R}^c \mid J_1 = j_1, L_0^d = \ell_0^d, L_0^s = \ell_0^s\}}{\mathbb{P}\{V_{k-\ell_{\max}^m+1:k-1} \in \mathcal{R}^c \mid J_1 = j_1, L_0^d = \ell_0^d, L_0^s = \ell_0^s\}} \\
 &= \underbrace{\left[\prod_{k=1}^{j_1 - \ell_{\max}^m} \frac{\mathbb{P}\{V_{k:k+\ell_{\max}^m-1} \in \mathcal{R}^c \mid J_1 = j_1, L_0^d = \ell_0^d, L_0^s = \ell_0^s\}}{\mathbb{P}\{V_{k+1:k+\ell_{\max}^m-1} \in \mathcal{R}^c \mid J_1 = j_1, L_0^d = \ell_0^d, L_0^s = \ell_0^s\}} \right]}_{\triangleq \Lambda_{\text{pnl}}(j_1, \ell_0^d, \ell_0^s)} \mathbb{P}\{V_{j_1 - \ell_{\max}^m + 1:j_1} \in \mathcal{R}^c \mid J_1 = j_1, L_0^d = \ell_0^d, L_0^s = \ell_0^s\}
 \end{aligned} \tag{11}$$

in the numerator is a ℓ_{\max}^m -joint probability, and each of the $j_1 - \ell_{\max}^m$ terms in the denominator is a $(\ell_{\max}^m - 1)$ -joint probability.¹³ Different terms in the numerator correspond to different segments of length ℓ_{\max}^m , which are time-shifted versions of one another (see Fig. 6b). Similarly, different terms in the denominator correspond to different segments of length $\ell_{\max}^m - 1$, which are also time-shifted versions of one another (see Fig. 6c). In general, these joint-probability terms need to be obtained numerically.¹⁴

B. Derivation for p_{det}

A similar approach to the previous section gives

$$\begin{aligned} p_{\text{det}} &= \mathbb{P}\{V_{1:J_1-1} \in \mathcal{R}^c, V_{J_1} \in \mathcal{R}\} \\ &= \sum_{\ell_0^d=1}^{\ell_{\max}^d} \sum_{\ell_0^s=0}^{\ell_{\max}^s} \sum_{j_1=1}^{\ell_0^d+\ell_0^s+\ell_{\max}^m} \mathbb{P}\{V_{1:J_1-1} \in \mathcal{R}^c, V_{J_1} \in \mathcal{R} \mid \\ &\quad J_1 = j_1, L_0^d = \ell_0^d, L_0^s = \ell_0^s\} \\ &\quad \times \left(\frac{1}{\ell_0^d + \ell_0^s + \ell_{\max}^m} \right) \mathbb{P}\{L_0^d = \ell_0^d\} \mathbb{P}\{L_0^s = \ell_0^s\}. \end{aligned}$$

The conditional probability for $j_1 = 1$ is given by

$$\begin{aligned} &\mathbb{P}\{V_{1:0} \in \mathcal{R}^c, V_1 \in \mathcal{R} \mid J_1 = 1, L_0^d = \ell_0^d, L_0^s = \ell_0^s\} \\ &\triangleq \mathbb{P}\{V_1 \in \mathcal{R} \mid J_1 = 1, L_0^d = \ell_0^d, L_0^s = \ell_0^s\} \\ &= 1 - \mathbb{P}\{V_1 \in \mathcal{R}^c \mid J_1 = 1, L_0^d = \ell_0^d, L_0^s = \ell_0^s\}, \end{aligned}$$

where the term on the right-hand side has already appeared during the evaluation of p_{nal} . The conditional probability for

¹³We use the term *k-joint probability* to refer to a joint probability of k random variables.

¹⁴Each probability term in (11) can be obtained by integrating the conditional joint pdf of V_k 's over the corresponding region.

$2 \leq j_1 \leq \ell_{\max}^m$ can be written as

$$\begin{aligned} &\mathbb{P}\{V_{1:J_1-1} \in \mathcal{R}^c, V_{J_1} \in \mathcal{R} \mid J_1 = j_1, L_0^d = \ell_0^d, L_0^s = \ell_0^s\} \\ &= \mathbb{P}\{V_{1:J_1-1} \in \mathcal{R}^c \mid J_1 = j_1, L_0^d = \ell_0^d, L_0^s = \ell_0^s\} \\ &\quad - \mathbb{P}\{V_{1:J_1} \in \mathcal{R}^c \mid J_1 = j_1, L_0^d = \ell_0^d, L_0^s = \ell_0^s\}. \end{aligned} \quad (12)$$

The second probability term on the right-hand side has appeared during the evaluation of p_{nal} . The first probability has not appeared before and needs to be evaluated. The conditional probability for $j_1 \geq \ell_{\max}^m + 1$ can be written as (13) at the bottom of the page, where all terms have already appeared in (11) during the evaluation of p_{nal} .¹⁵

C. Derivation for $p_{\text{nal-nal}}$

A similar approach to the previous section gives

$$\begin{aligned} p_{\text{nal-nal}} &= \mathbb{P}\{V_{1:J_2} \in \mathcal{R}^c\} \\ &= \sum_{\ell_0^d=1}^{\ell_{\max}^d} \sum_{\ell_0^s=0}^{\ell_{\max}^s} \sum_{j_1=1}^{\ell_0^d+\ell_0^s+\ell_{\max}^m} \sum_{\ell_1^d=1}^{\ell_{\max}^d} \sum_{\ell_1^s=0}^{\ell_{\max}^s} \mathbb{P}\{V_{1:J_2} \in \mathcal{R}^c \mid \\ &\quad J_1 = j_1, L_0^d = \ell_0^d, L_0^s = \ell_0^s, L_1^d = \ell_1^d, L_1^s = \ell_1^s\} \\ &\quad \times \left(\frac{1}{\ell_0^d + \ell_0^s + \ell_{\max}^m} \right) \mathbb{P}\{L_0^d = \ell_0^d\} \mathbb{P}\{L_0^s = \ell_0^s\} \\ &\quad \times \mathbb{P}\{L_1^d = \ell_1^d\} \mathbb{P}\{L_1^s = \ell_1^s\}. \end{aligned}$$

The conditional probability can be obtained using similar steps leading to (11), resulting in (14) at the bottom of the page, where $j_2 \triangleq j_1 + \ell_1^d + \ell_1^s + \ell_{\max}^m$.¹⁶

Equation (14) can be interpreted with the help of Fig. 7 as follows. The condition $\{J_1 = j_1, L_0^d = \ell_0^d, L_0^s = \ell_0^s, L_1^d =$

¹⁵The first probability expression in the bracket is the last joint-probability term in the *denominator* of $\Lambda_{\text{pnal}}(j_1, \ell_0^d, \ell_0^s)$ in (11). The second probability expression in the bracket is the last joint-probability term in the *numerator* of (11).

¹⁶Recall that $J_2 = j_1 + \ell_1^d + \ell_1^s + \ell_{\max}^m$ when conditioned on $J_1 = j_1$, $L_1^d = \ell_1^d$, and $L_1^s = \ell_1^s$.

$$\begin{aligned} &\mathbb{P}\{V_{1:J_1-1} \in \mathcal{R}^c, V_{J_1} \in \mathcal{R} \mid J_1 = j_1, L_0^d = \ell_0^d, L_0^s = \ell_0^s\} \\ &= \left[\prod_{k=1}^{j_1-1} \frac{\mathbb{P}\{V_k: k+\ell_{\max}^m-1 \in \mathcal{R}^c \mid J_1 = j_1, L_0^d = \ell_0^d, L_0^s = \ell_0^s\}}{\mathbb{P}\{V_{k+1}: k+\ell_{\max}^m-1 \in \mathcal{R}^c \mid J_1 = j_1, L_0^d = \ell_0^d, L_0^s = \ell_0^s\}} \right] \\ &\quad \times \mathbb{P}\{V_{J_1-\ell_{\max}^m+1: J_1-1} \in \mathcal{R}^c, V_{J_1} \in \mathcal{R} \mid J_1 = j_1, L_0^d = \ell_0^d, L_0^s = \ell_0^s\} \\ &= \Lambda_{\text{pnal}}(j_1, \ell_0^d, \ell_0^s) \left[\mathbb{P}\{V_{J_1-\ell_{\max}^m+1: J_1-1} \in \mathcal{R}^c \mid J_1 = j_1, L_0^d = \ell_0^d, L_0^s = \ell_0^s\} \right. \\ &\quad \left. - \mathbb{P}\{V_{J_1-\ell_{\max}^m+1: J_1} \in \mathcal{R}^c \mid J_1 = j_1, L_0^d = \ell_0^d, L_0^s = \ell_0^s\} \right] \quad (13) \end{aligned}$$

$$\begin{aligned} &\mathbb{P}\{V_{1:j_2} \in \mathcal{R}^c \mid J_1 = j_1, L_0^d = \ell_0^d, L_0^s = \ell_0^s, L_1^d = \ell_1^d, L_1^s = \ell_1^s\} \\ &= \left[\prod_{k=1}^{j_2-\ell_{\max}^m} \frac{\mathbb{P}\{V_k: k+\ell_{\max}^m-1 \in \mathcal{R}^c \mid J_1 = j_1, L_0^d = \ell_0^d, L_0^s = \ell_0^s, L_1^d = \ell_1^d, L_1^s = \ell_1^s\}}{\mathbb{P}\{V_{k+1}: k+\ell_{\max}^m-1 \in \mathcal{R}^c \mid J_1 = j_1, L_0^d = \ell_0^d, L_0^s = \ell_0^s, L_1^d = \ell_1^d, L_1^s = \ell_1^s\}} \right] \\ &\quad \triangleq \Lambda_{\text{pnal-nal}}(j_1, \ell_0^d, \ell_0^s, \ell_1^d, \ell_1^s) \\ &\quad \times \mathbb{P}\{V_{j_2-\ell_{\max}^m+1: j_2} \in \mathcal{R}^c \mid J_1 = j_1, L_0^d = \ell_0^d, L_0^s = \ell_0^s, L_1^d = \ell_1^d, L_1^s = \ell_1^s\} \quad (14) \end{aligned}$$

$\ell_1^d, L_1^s = \ell_1^s$ indicates that the segment of the observed symbols consists of (a) the last j_1 symbols of an MSS with length $\ell_0^d + \ell_0^s + \ell_{\max}^m$, (b) all symbols of the next MSS with length $\ell_1^d + \ell_1^s + \ell_{\max}^m$, and (c) $\ell_{\max}^m - 1$ marker symbols (see Fig. 7a). These observed symbols generate a total of j_2 decision variables. Each of the $j_2 - \ell_{\max}^m + 1$ terms in the numerator is a ℓ_{\max}^m -joint probability, and each of the $j_2 - \ell_{\max}^m$ terms in the denominator is a $(\ell_{\max}^m - 1)$ -joint probability. Different terms in the numerator correspond to different segments of length ℓ_{\max}^m , which are time-shifted versions of one another (see Fig. 7b). Similarly, different terms in the denominator correspond to different segments of length $\ell_{\max}^m - 1$, which are also time-shifted versions of one another (see Fig. 7c). In general, these joint-probability terms need to be obtained numerically.

By comparing Fig. 7 and Fig. 6, it will be apparent that most of the ℓ_{\max}^m -joint probabilities and $(\ell_{\max}^m - 1)$ -joint probabilities in (14) have already appeared in (11) for the evaluation of p_{nal} . The remaining joint probability terms need to be evaluated, and these terms correspond to the segments near the boundary of the MSSs. Hence, the effort to obtain $p_{\text{nal-nal}}$ after we have obtained p_{nal} is minimal from a numerical point of view.

D. Derivation for $p_{\text{nal-det}}$

A similar approach to the previous case gives

$$\begin{aligned}
 p_{\text{nal-det}} &= \mathbb{P}\{V_{1:J_2-1} \in \mathcal{R}^c, V_{J_2} \in \mathcal{R}\} \\
 &= \sum_{\ell_0^d=1}^{\ell_{\max}^d} \sum_{\ell_0^s=0}^{\ell_{\max}^s} \sum_{j_1=1}^{\ell_0^d+\ell_0^s+\ell_{\max}^m} \sum_{\ell_1^d=1}^{\ell_{\max}^d} \sum_{\ell_1^s=0}^{\ell_{\max}^s} \mathbb{P}\{V_{1:J_2-1} \in \mathcal{R}^c, V_{J_2} \in \mathcal{R} \mid \\
 &\quad J_1 = j_1, L_0^d = \ell_0^d, L_0^s = \ell_0^s, L_1^d = \ell_1^d, L_1^s = \ell_1^s\}
 \end{aligned}$$

$$\begin{aligned}
 &\mathbb{P}\{V_{1:j_2-1} \in \mathcal{R}^c, V_{j_2} \in \mathcal{R} \mid J_1 = j_1, L_0^d = \ell_0^d, L_0^s = \ell_0^s, L_1^d = \ell_1^d, L_1^s = \ell_1^s\} \\
 &= \Lambda_{\text{pnal-nal}}(j_1, \ell_0^d, \ell_0^s, \ell_1^d, \ell_1^s) \mathbb{P}\{V_{j_2-\ell_{\max}^m+1:j_2-1} \in \mathcal{R}^c, V_{j_2} \in \mathcal{R} \mid J_1 = j_1, L_0^d = \ell_0^d, L_0^s = \ell_0^s, L_1^d = \ell_1^d, L_1^s = \ell_1^s\} \\
 &= \Lambda_{\text{pnal-nal}}(j_1, \ell_0^d, \ell_0^s, \ell_1^d, \ell_1^s) \left[\mathbb{P}\{V_{j_2-\ell_{\max}^m+1:j_2-1} \in \mathcal{R}^c \mid J_1 = j_1, L_0^d = \ell_0^d, L_0^s = \ell_0^s, L_1^d = \ell_1^d, L_1^s = \ell_1^s\} \right. \\
 &\quad \left. - \mathbb{P}\{V_{j_2-\ell_{\max}^m+1:j_2} \in \mathcal{R}^c \mid J_1 = j_1, L_0^d = \ell_0^d, L_0^s = \ell_0^s, L_1^d = \ell_1^d, L_1^s = \ell_1^s\} \right] \quad (15)
 \end{aligned}$$

$$\begin{aligned}
 c_{\text{nal}} &= \mathbb{P}\{V_{J_2+1:J_3} \in \mathcal{R}^c \mid V_{J_2-\ell_{\max}^m+2:J_2} \in \mathcal{R}^c\} \\
 &= \sum_{\ell_1^d=1}^{\ell_{\max}^d} \sum_{\ell_1^s=0}^{\ell_{\max}^s} \sum_{\ell_2^d=1}^{\ell_{\max}^d} \sum_{\ell_2^s=0}^{\ell_{\max}^s} \frac{\mathbb{P}\{V_{J_2-\ell_{\max}^m+2:J_3} \in \mathcal{R}^c \mid L_1^d = \ell_1^d, L_1^s = \ell_1^s, L_2^d = \ell_2^d, L_2^s = \ell_2^s\}}{\mathbb{P}\{V_{J_2-\ell_{\max}^m+2:J_2} \in \mathcal{R}^c \mid L_1^d = \ell_1^d, L_1^s = \ell_1^s, L_2^d = \ell_2^d, L_2^s = \ell_2^s\}} \\
 &\quad \times \mathbb{P}\{L_1^d = \ell_1^d\} \mathbb{P}\{L_1^s = \ell_1^s\} \mathbb{P}\{L_2^d = \ell_2^d\} \mathbb{P}\{L_2^s = \ell_2^s\} \quad (16)
 \end{aligned}$$

$$\begin{aligned}
 c_{\text{nal}} &= \sum_{\ell_1^d=1}^{\ell_{\max}^d} \sum_{\ell_1^s=0}^{\ell_{\max}^s} \sum_{\ell_2^d=1}^{\ell_{\max}^d} \sum_{\ell_2^s=0}^{\ell_{\max}^s} \frac{\mathbb{P}\{W_{1:J_3-J_2+\ell_{\max}^m-1} \in \mathcal{R}^c \mid L_1^d = \ell_1^d, L_1^s = \ell_1^s, L_2^d = \ell_2^d, L_2^s = \ell_2^s\}}{\mathbb{P}\{W_{1:\ell_{\max}^m-1} \in \mathcal{R}^c \mid L_1^d = \ell_1^d, L_1^s = \ell_1^s, L_2^d = \ell_2^d, L_2^s = \ell_2^s\}} \\
 &\quad \times \mathbb{P}\{L_1^d = \ell_1^d\} \mathbb{P}\{L_1^s = \ell_1^s\} \mathbb{P}\{L_2^d = \ell_2^d\} \mathbb{P}\{L_2^s = \ell_2^s\} \quad (17)
 \end{aligned}$$

$$\begin{aligned}
 &\times \left(\frac{1}{\ell_0^d + \ell_0^s + \ell_{\max}^m} \right) \mathbb{P}\{L_0^d = \ell_0^d\} \mathbb{P}\{L_0^s = \ell_0^s\} \\
 &\times \mathbb{P}\{L_1^d = \ell_1^d\} \mathbb{P}\{L_1^s = \ell_1^s\},
 \end{aligned}$$

where the conditional probability can be obtained numerically from the expansion (15) at the bottom of the page, for $j_2 \triangleq j_1 + \ell_1^d + \ell_1^s + \ell_{\max}^m$. All terms in (15) have appeared in (14) for the evaluation of $p_{\text{nal-nal}}$.¹⁷ Hence, the effort to obtain $p_{\text{nal-det}}$ after we have obtained $p_{\text{nal-nal}}$ is minimal from a numerical point of view.

E. Derivation for c_{nal}

We write c_{nal} as given by (16) at the bottom of the page.

To simplify the index, we let $W_j \triangleq V_{j+J_2-\ell_{\max}^m+1}$, for $j \geq 1$. Then, c_{nal} is given by (17) at the bottom of the page. The ratio of conditional probabilities in the summation can be obtained by expanding the numerator using similar steps leading to (11): for the length $n \triangleq \ell_2^d + \ell_2^s + 2\ell_{\max}^m - 1$,¹⁸

$$\begin{aligned}
 &\frac{\mathbb{P}\{W_{1:n} \in \mathcal{R}^c \mid L_1^d = \ell_1^d, L_1^s = \ell_1^s, L_2^d = \ell_2^d, L_2^s = \ell_2^s\}}{\mathbb{P}\{W_{1:\ell_{\max}^m-1} \in \mathcal{R}^c \mid L_1^d = \ell_1^d, L_1^s = \ell_1^s, L_2^d = \ell_2^d, L_2^s = \ell_2^s\}} \\
 &= \Lambda_{\text{cnal}}(\ell_1^d, \ell_1^s, \ell_2^d, \ell_2^s) \mathbb{P}\{W_{n-\ell_{\max}^m+1:n} \in \mathcal{R}^c \mid \\
 &\quad L_1^d = \ell_1^d, L_1^s = \ell_1^s, L_2^d = \ell_2^d, L_2^s = \ell_2^s\}, \quad (18)
 \end{aligned}$$

where $\Lambda_{\text{cnal}}(\ell_1^d, \ell_1^s, \ell_2^d, \ell_2^s)$ is given by (19) at the bottom of the next page.

Equation (18) can be interpreted with the help of Fig. 8 as follows. The condition $\{L_1^d = \ell_1^d, L_1^s = \ell_1^s, L_2^d = \ell_2^d, L_2^s = \ell_2^s\}$ indicates that the segment of observed symbols consists of (a)

¹⁷The first probability expression in the bracket is the last joint-probability term in the *denominator* of (14). The second probability expression in the bracket is the last joint-probability term in the *numerator* of (14).

¹⁸Recall that $J_3 - J_2 = T_2 = \ell_2^d + \ell_2^s + \ell_{\max}^m$ when conditioned on $L_2^d = \ell_2^d$ and $L_2^s = \ell_2^s$.

the last $\ell_{\max}^m - 1$ symbols from an MSS, (b) entire $\ell_2^d + \ell_2^s + \ell_{\max}^m$ symbols from the next MSS, and (c) $\ell_{\max}^m - 1$ marker symbols (see Fig. 8a). These observed symbols generate a total of n decision variables. Each of the $n - \ell_{\max}^m + 1$ terms in the numerator is a ℓ_{\max}^m -joint probability, and each of the $n - \ell_{\max}^m + 1$ terms in the denominator is a $(\ell_{\max}^m - 1)$ -joint probability. Different terms in the numerator correspond to different segments of length ℓ_{\max}^m , which are time-shifted versions of one another (see Fig. 8b). Similarly, different terms in the denominator correspond to different segments of length $\ell_{\max}^m - 1$, which are also time-shifted versions of one another (see Fig. 8c). In general, these joint-probability terms need to be obtained numerically.

A comparison of Fig. 8 and Fig. 7 shows that all ℓ_{\max}^m -joint probabilities and $(\ell_{\max}^m - 1)$ -joint probabilities in (18) and (19) have already appeared in (14) for the evaluation of $p_{\text{nal-nal}}$. Hence, the effort to obtain c_{nal} after we have obtained $p_{\text{nal-nal}}$ is minimal from a numerical point of view.

F. Derivation for c_{det}

A similar approach to the previous section gives (20) at the bottom of the page, where $n \triangleq n(\ell_2^d, \ell_2^s) = \ell_2^d + \ell_2^s + 2\ell_{\max}^m - 1$ and $W_j \triangleq V_{j+J_2-\ell_{\max}^m+1}$. The ratio of conditional probabilities in the summation can be written as (21) at the bottom of the page, where all terms in the right-hand side of (21) have already appeared in (18) for the evaluation of c_{nal} .¹⁹ Hence, the effort to obtain c_{det} after we have obtained c_{nal} is minimal from a numerical point of view.

¹⁹The first probability expression in the bracket is the last joint-probability term in the denominator of (19). The second probability expression in the bracket is the last joint-probability term in (18).

VI. COMPUTATION TIME

This section assesses the computation time as a function of system parameters, ℓ_{\max}^m , ℓ_{\max}^d , and ℓ_{\max}^s .

Computation time T_{comp} required for evaluating the transition probabilities arises from two subtasks. The first subtask is to evaluate the joint probability terms that appear in the expressions for the transition probabilities. The second subtask is to multiply these joint probability terms and sum them during the evaluation of the transition probabilities. Total computation time equals computation time $T_{\text{comp}}^{(1)}$ for the first subtask plus the computation time $T_{\text{comp}}^{(2)}$ for the second subtask.

Computation time for the first subtask depends on the number of distinct joint probabilities and is given by

$$T_{\text{comp}}^{(1)} = \sum_{k=1}^{\ell_{\max}^m} \tilde{N}(k) E(k), \quad (22)$$

where $E(k)$ denotes the computation time of a k -joint probability and $\tilde{N}(k)$ denotes the number of k -joint probabilities required to evaluate the transition probabilities. If the transition probabilities are derived according to the previous section, the value of $\tilde{N}(k)$ satisfies (see Appendix F)

$$2 \leq \tilde{N}(k) \leq 2k + 1, \quad \text{for } 1 \leq k \leq \ell_{\max}^m - 2, \quad (23a)$$

$$3\ell_{\max}^m - 2 \leq \tilde{N}(\ell_{\max}^m - 1) \leq 5\ell_{\max}^m - 4, \quad (23b)$$

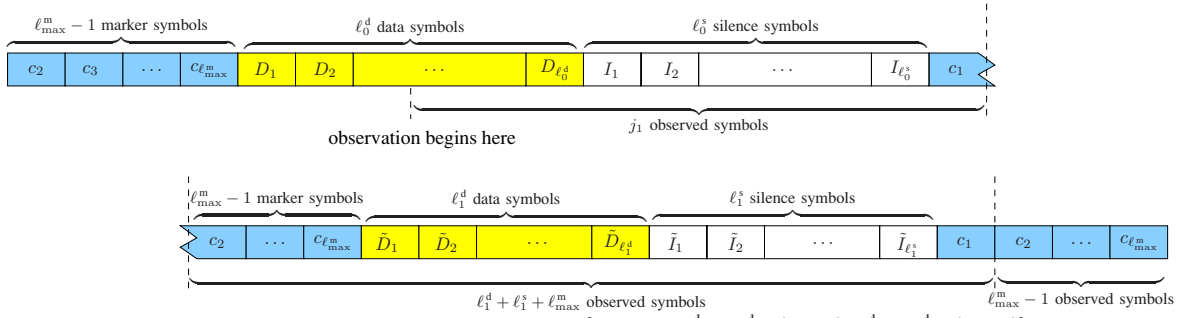
$$3\ell_{\max}^m - 1 \leq \tilde{N}(\ell_{\max}^m) \leq 5\ell_{\max}^m - 2. \quad (23c)$$

According to the appendix, the left inequalities are satisfied with equality if $L_i^s = 0$, a typical case for continuous transmission without any idle fill character. The right inequalities

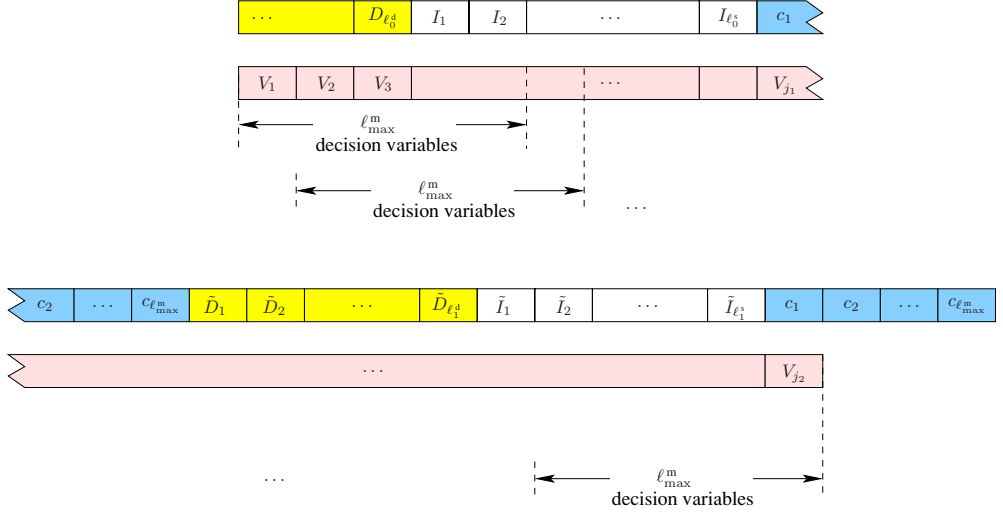
$$\Lambda_{\text{cna}}(\ell_1^d, \ell_1^s, \ell_2^d, \ell_2^s) \triangleq \frac{1}{\mathbb{P}\{W_{1:\ell_{\max}^m-1} \in \mathcal{R}^c \mid L_1^d = \ell_1^d, L_1^s = \ell_1^s, L_2^d = \ell_2^d, L_2^s = \ell_2^s\}} \times \left[\prod_{k=1}^{n-\ell_{\max}^m} \frac{\mathbb{P}\{W_k:k+\ell_{\max}^m-1 \in \mathcal{R}^c \mid L_1^d = \ell_1^d, L_1^s = \ell_1^s, L_2^d = \ell_2^d, L_2^s = \ell_2^s\}}{\mathbb{P}\{W_{k+1}:k+\ell_{\max}^m-1 \in \mathcal{R}^c \mid L_1^d = \ell_1^d, L_1^s = \ell_1^s, L_2^d = \ell_2^d, L_2^s = \ell_2^s\}} \right] \quad (19)$$

$$\begin{aligned} c_{\text{det}} &= \mathbb{P}\{V_{J_2+1:J_3-1} \in \mathcal{R}^c, V_{J_3} \in \mathcal{R} \mid V_{J_2-\ell_{\max}^m+2:J_2} \in \mathcal{R}^c\} \\ &= \sum_{\ell_1^d=1}^{\ell_{\max}^d} \sum_{\ell_1^s=0}^{\ell_{\max}^s} \sum_{\ell_2^d=1}^{\ell_{\max}^d} \sum_{\ell_2^s=0}^{\ell_{\max}^s} \frac{\mathbb{P}\{W_{1:n-1} \in \mathcal{R}^c, W_n \in \mathcal{R} \mid L_1^d = \ell_1^d, L_1^s = \ell_1^s, L_2^d = \ell_2^d, L_2^s = \ell_2^s\}}{\mathbb{P}\{W_{1:\ell_{\max}^m-1} \in \mathcal{R}^c \mid L_1^d = \ell_1^d, L_1^s = \ell_1^s, L_2^d = \ell_2^d, L_2^s = \ell_2^s\}} \\ &\quad \times \mathbb{P}\{L_1^d = \ell_1^d\} \mathbb{P}\{L_1^s = \ell_1^s\} \mathbb{P}\{L_2^d = \ell_2^d\} \mathbb{P}\{L_2^s = \ell_2^s\} \end{aligned} \quad (20)$$

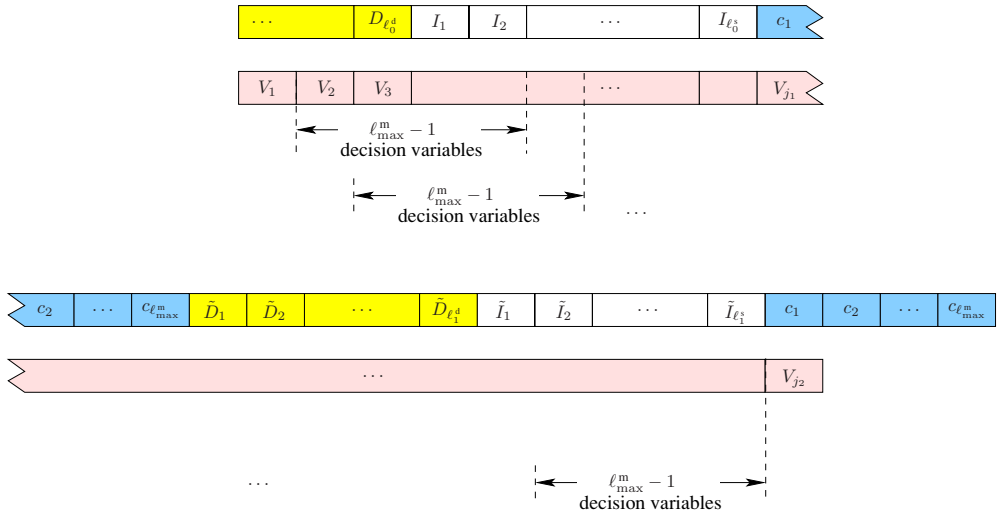
$$\begin{aligned} &\frac{\mathbb{P}\{W_{1:n-1} \in \mathcal{R}^c, W_n \in \mathcal{R} \mid L_1^d = \ell_1^d, L_1^s = \ell_1^s, L_2^d = \ell_2^d, L_2^s = \ell_2^s\}}{\mathbb{P}\{W_{1:\ell_{\max}^m-1} \in \mathcal{R}^c \mid L_1^d = \ell_1^d, L_1^s = \ell_1^s, L_2^d = \ell_2^d, L_2^s = \ell_2^s\}} \\ &= \Lambda_{\text{cna}}(\ell_1^d, \ell_1^s, \ell_2^d, \ell_2^s) \left[\mathbb{P}\{W_{n-\ell_{\max}^m+1:n-1} \in \mathcal{R}^c \mid L_1^d = \ell_1^d, L_1^s = \ell_1^s, L_2^d = \ell_2^d, L_2^s = \ell_2^s\} \right. \\ &\quad \left. - \mathbb{P}\{W_{n-\ell_{\max}^m+1:n} \in \mathcal{R}^c \mid L_1^d = \ell_1^d, L_1^s = \ell_1^s, L_2^d = \ell_2^d, L_2^s = \ell_2^s\} \right] \quad (21) \end{aligned}$$



(a) Sequence of symbols satisfying the condition $\{J_1 = j_1, L_0^d = \ell_0^d, L_0^s = \ell_0^s, L_1^d = \ell_1^d, L_1^s = \ell_1^s\}$



(b) Blocks of length ℓ_{\max}^m , each of which corresponds to a different ℓ_{\max}^m -joint probability term in the numerator



(c) Blocks of length $\ell_{\max}^m - 1$, each of which corresponds to a different $(\ell_{\max}^m - 1)$ -joint probability term in the denominator

Fig. 7. Pictorial representation of the MSS helps to aid the interpretation of equation (14).

are satisfied with equality if $L_i^s \geq 2\ell_{\max}^m - 2$, a typical case for a transmission with large number of idle fill characters or a bursty transmission with long silent periods. The value of $E(k)$ depends on a specific application. For example, an

exponential function, $E(k) = c^k$ for a constant $c > 1$, is a reasonable model for computation time of a k -nested integration using a conventional approach [49, p. 161]. In that

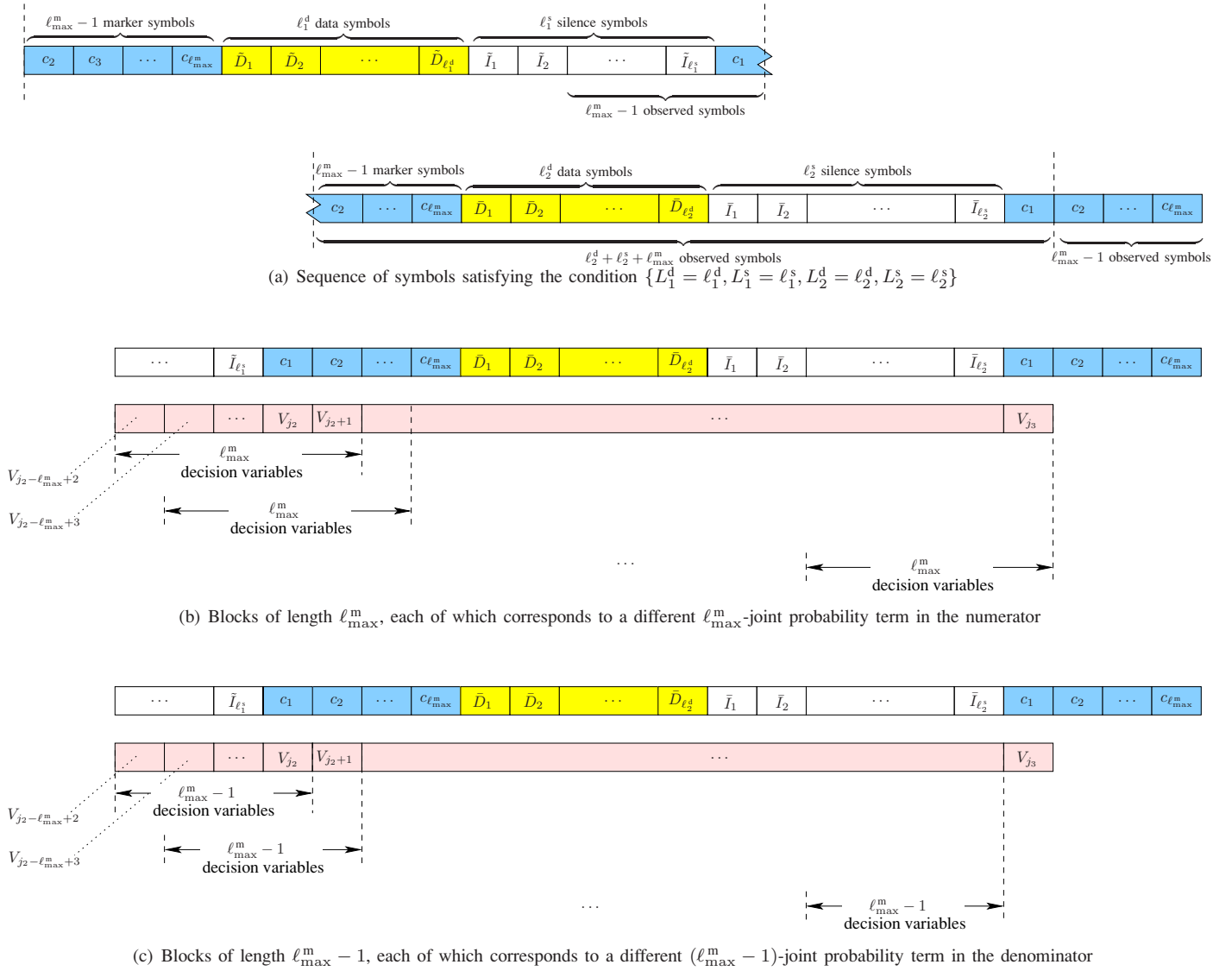


Fig. 8. Pictorial representation of the MSSs helps to aid the interpretation of equation (18).

case, $T_{\text{comp}}^{(1)}$ in (22) becomes [50, eq. 0.113]

$$T_{\text{comp}}^{(1)} = O\left(\ell_{\max}^m c^{\ell_{\max}^m}\right),$$

which gives a computation time for the first subtask.

Computation time for the second subtask is dominated by time required to evaluate $p_{\text{na1-na1}}$. Hence,

$$T_{\text{comp}}^{(2)} = \begin{cases} O\left((\ell_{\max}^d)^2 (\ell_{\max}^d + \ell_{\max}^m)^2\right), & \text{if } \ell_{\max}^s = 0; \\ O\left((\ell_{\max}^d)^2 (\ell_{\max}^s)^2 (\ell_{\max}^d + \ell_{\max}^s + \ell_{\max}^m)^2\right), & \text{if } \ell_{\max}^s \geq \ell_{\max}^m - 1. \end{cases}$$

Therefore, total computation time is

$$T_{\text{comp}} = \begin{cases} O\left((\ell_{\max}^d)^2 (\ell_{\max}^d + \ell_{\max}^m)^2 + \ell_{\max}^m c^{\ell_{\max}^m}\right), & \text{if } \ell_{\max}^s = 0; \\ O\left((\ell_{\max}^d)^2 (\ell_{\max}^s)^2 (\ell_{\max}^d + \ell_{\max}^s + \ell_{\max}^m)^2 + \ell_{\max}^m c^{\ell_{\max}^m}\right), & \text{if } \ell_{\max}^s \geq \ell_{\max}^m - 1. \end{cases}$$

VII. NUMERICAL EXAMPLES

To illustrate our analytical framework developed in previous sections, we consider the simplest scenario, involving continuous transmission of binary symbols over the additive white Gaussian noise (AWGN) channel.

A. Case Study

Transmitted data symbols, $\{D_j\}$, are assumed to be i.i.d. and equally likely to take a value of -1 or $+1$. The length L_i^d of frame number i is uniform over the set, $\{\ell_{\min}^d, \ell_{\min}^d + 1, \dots, \ell_{\max}^d\}$, and $L_i^s = 0$. The transmitter injects a marker with good correlation properties into the beginning of each frame. The data and marker symbols are converted into waveforms for transmission, which are impaired by AWGN.

The frame synchronizer decides whether a marker begins at index j by considering two hypotheses. Let H_1 denote the hypothesis that a marker begins at index j , whereas H_0 denotes

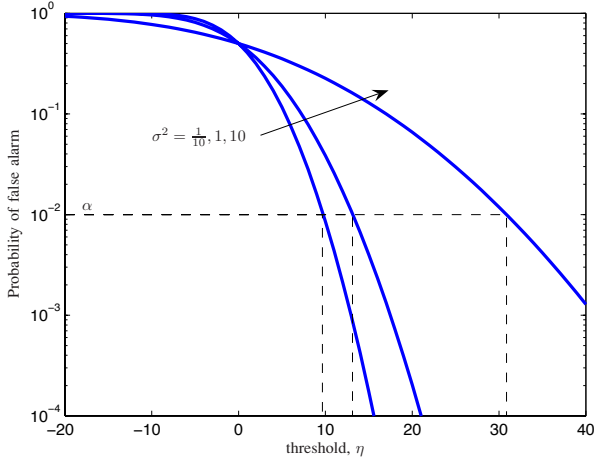


Fig. 9. The threshold is selected to achieve the probability of false alarm at a desired level, α . The figure shows $\alpha = 10^{-2}$ and the marker length $\ell_{\max}^m = 16$.

the hypothesis that a marker does not begin at index j :

$$\begin{aligned} H_1 : X_i &= c_{i-j+1} + N_i, \quad (i = j, j+1, \dots, j + \ell_{\max}^m - 1) \\ H_0 : X_i &= D_i + N_i, \quad (i = j, j+1, \dots, j + \ell_{\max}^m - 1). \end{aligned}$$

Here, $\{N_i\}$ are i.i.d. Gaussian random variables with zero mean and variance σ^2 . We eliminate the cases where there is a mixture of data and marker symbols from our hypothesis, since segments of well-designed markers should mimic a sequence of random data [37], [38].

We will employ a decision rule based on soft correlation with the decision function g_1 in (1). The threshold for decision rule, denoted by η , is chosen according to the Neyman-Pearson criteria [51, p. 216]. Hence, our decision rule becomes

$$V_j \triangleq \sum_{k=1}^{\ell_{\max}^m} c_k X_{j+k-1} \underset{H_0}{\overset{H_1}{\gtrless}} \eta.$$

B. Selection of Threshold

Let the random variable $H \in \{H_1, H_0\}$ denote the true hypothesis. Using Neyman-Pearson criteria, we select a threshold η such that the probability of false alarm equals a desired level, α :

$$\mathbb{P}\{V_j > \eta \mid H = H_0\} = \alpha. \quad (24)$$

We now evaluate the false alarm probability as follows.

Without loss of generality, we will set the time index $j = 1$. Under hypothesis $H = H_0$, decision variable V_1 involves a sum of i.i.d. Bernoulli random variables, $\sum_{k=1}^{\ell_{\max}^m} c_k D_k$, and a sum of normal random variables, $\sum_{k=1}^{\ell_{\max}^m} c_k N_k$. The probability of false alarm at a given threshold η equals [38, eq. (51)]

$$\begin{aligned} \mathbb{P}\{V_j > \eta \mid H = H_0\} \\ = \frac{1}{2^{\ell_{\max}^m}} \sum_{k=0}^{\ell_{\max}^m} \binom{\ell_{\max}^m}{k} Q\left(\frac{\eta - \ell_{\max}^m + 2k}{\sqrt{\sigma^2 \ell_{\max}^m}}\right), \end{aligned}$$

where $Q(x)$ is Gaussian Q -function [52, eq. 2.1–97]. We

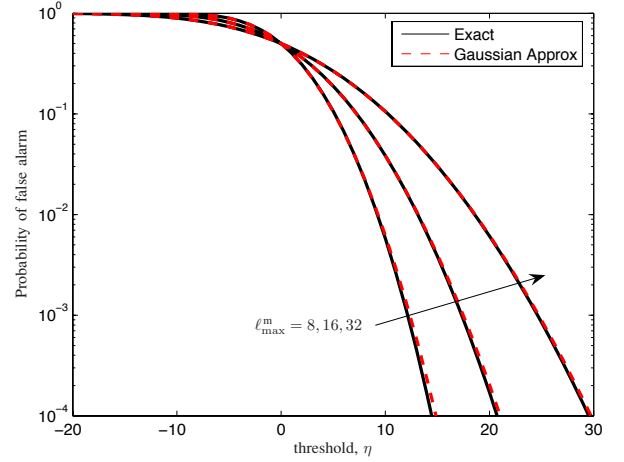


Fig. 10. The Gaussian approximation can be used to approximate the probability of false alarm ($\sigma^2 = 1$).

then obtain η by numerically solving the nonlinear equation (24) using a technique such as the bisection method. The probability of false alarm for various σ^2 is depicted in Fig. 9.

Remark 1: The bisection method requires an initial point η_0 to begin the iteration. One approach to select a good initial point is to approximate V_j by a Gaussian random variable. This approximation is motivated by the central limit theorem. Mathematically, for large ℓ_{\max}^m the false alarm probability, $\mathbb{P}\{V_j > \eta \mid H = H_0\}$, is approximated by

$$Q\left(\frac{\eta}{\sqrt{\ell_{\max}^m(1 + \sigma^2)}}\right).$$

Under this approximation, the initial point is given by

$$\eta_0 = Q^{-1}(\alpha) \sqrt{\ell_{\max}^m(1 + \sigma^2)},$$

which is easy to obtain using standard mathematical packages. The Gaussian approximation turns out to be very good (Fig. 10), implying that the bisection method will terminate in a few steps.

Remark 2: To obtain the transition probabilities, we follow the approach described in Sec. V. Each joint probability term in that section is obtained by conditioning on data symbols, if applicable, and then integrating the joint pdf of the Gaussian random variables over the appropriate region, defined by the threshold.²⁰ As an example, a joint probability term that needs to be evaluated is

$$\mathbb{P}\{W_1 \leq \eta, W_2 \leq \eta, \dots, W_{\ell_{\max}^m} \leq \eta\}$$

where

$$W_j = \sum_{k=1}^{\ell_{\max}^m} c_k (D_{k+j-1} + N_{k+j-1}) \quad (j = 1, 2, 3, \dots, \ell_{\max}^m).$$

²⁰If the joint probability term is generated by the marker symbols only, then the conditioning is unnecessary.

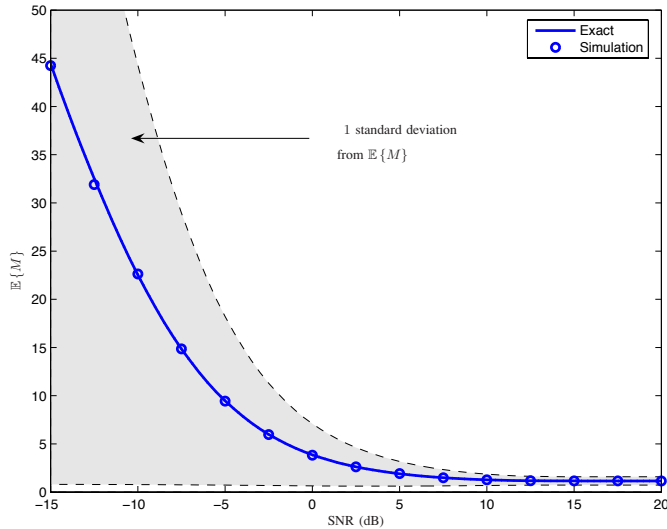


Fig. 11. The expected number of MSSs required for a correct acquisition measures the amount of time to complete frame synchronization.

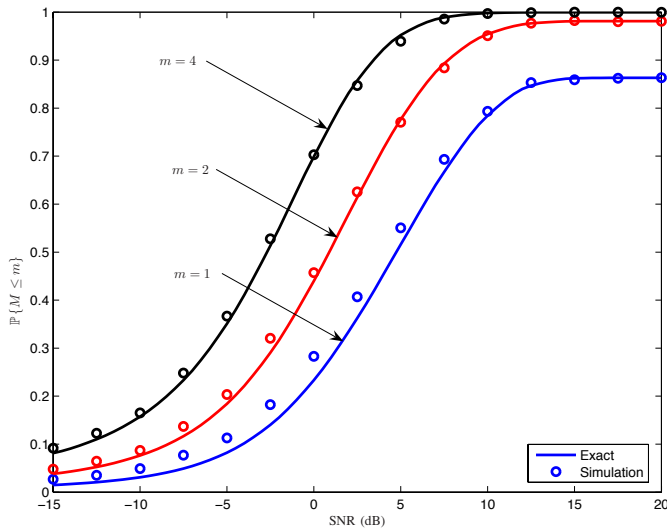


Fig. 12. As the duration m to acquire the marker increases, the probability of correct acquisition within the given duration increases.

To evaluate this probability, we write

$$\begin{aligned} & \mathbb{P}\{W_1 \leq \eta, W_2 \leq \eta, \dots, W_{\ell_{\max}^m} \leq \eta\} \\ &= \mathbb{E}\{\mathbb{P}\{W_1 \leq \eta, W_2 \leq \eta, \dots, W_{\ell_{\max}^m} \leq \eta \mid \\ & \quad D_1, D_2, \dots, D_{2\ell_{\max}^m - 1}\}\}, \end{aligned}$$

where the expectation is over the data symbols $\{D_j\}$. Conditioned on $\{D_j = d_j\}$ for $d_j \in \{-1, +1\}$, the random vector $(W_1, W_2, \dots, W_{\ell_{\max}^m})$ has a multivariate normal distribution, whose cumulative density function (cdf) can be obtained efficiently using, for example, the method in [53].²¹

C. Discussion

For the purpose of illustration, we consider a false alarm level of $\alpha = 1\%$, a marker of length $\ell_{\max}^m = 8$, and

²¹When ℓ_{\max}^m is large, the conditioning on $\{D_j\}$ may be too time-consuming. In that case, one may consider appropriate approximations.

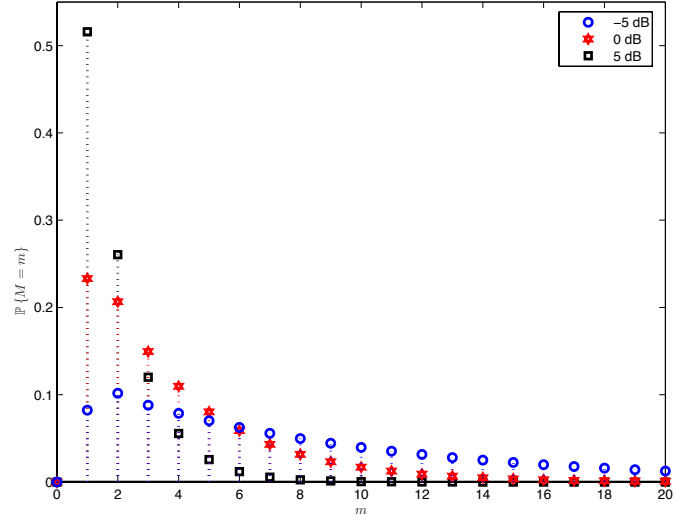


Fig. 13. The pmf of M is obtained from the performance metric $\mathbb{P}\{M \leq m\}$.

a frame length L_i^d that is uniform on $\{30, 31, \dots, 40\}$. Marker symbols are selected to be $(c_1, \dots, c_8) = (+1, -1, +1, +1, +1, -1, -1, -1)$ to ensure good correlation properties [10]. Using these parameters, we evaluate the performance metrics in Secs. III and IV.

Figure 11 shows the expected time to complete the marker acquisition as a function of the signal to noise ratio (SNR), $1/\sigma^2$. The expected time decreases with an increase in SNR as one would expect and reaches an asymptotic value, which is slightly greater than 1 in a high SNR regime.²² This behavior can be attributed to the fact that the errors can still occur due to the data symbols replicating the marker. To eliminate this type of decision error, the transmitter must modify the sequence of transmitted symbols, for example, using an approach similar to [54, p. 88].²³

Figure 12 shows the probability of correct acquisition within a given duration, measured in terms of the number m of MSSs. For the purpose of illustration, we consider $m = 1, 2, 4$. The probability of correct acquisition increases with m as one would expect, indicating that the longer the duration spent to detect a marker, the more likely that the marker acquisition will be correct. The probabilities $\mathbb{P}\{M \leq m\}$ in the high SNR regime are related to the events of data symbols replicating the marker. In Figs. 11–12, we also report the simulation results, which confirm the validity of our analysis.

The performance metric $\mathbb{P}\{M \leq m\}$ can be used to obtain the probability mass function (pmf) of M as well as the moments of M . For illustration purposes, we plot the pmf of M in Fig. 13 and the standard deviation of M as a shaded area around $\mathbb{E}\{M\}$ in Fig. 11.²⁴ Notice in Fig. 13 that the pmf of M for low SNR is spread, thus resulting in a large standard deviation as can be observed in Fig. 11.

VIII. CONCLUSION

Frame synchronization is important for packet transmission, especially in a network of cognitive radios. This paper focuses on both the continuous transmission of variable-length frames and bursty transmission of frames, which arise, for example, in multimedia encoded video streaming. The paper puts forth important performance metrics, namely the expected time to complete frame synchronization and the probability of correct acquisition within a given duration. The first metric is suitable for characterizing performance of transmission systems without delay constraints, while the second one is suitable for systems with delay constraints. We derive these performance metrics using renewal theory.

The strength of our approach is that these metrics can be expressed in terms of a few parameters, which we refer to as the transition probabilities. The transition probabilities depend on the SNR, the decision rule, and the fading conditions. We discuss approaches to obtain the transition probabilities numerically. Once the transition probabilities have been obtained for a given SNR, they can be used to evaluate the performance of a frame synchronization system.

To demonstrate an application of our results, we consider a simple example, involving continuous transmission in the AWGN channel. We use a soft decision rule and a threshold test for detecting a marker, where the threshold is selected according to the Neyman-Pearson criteria. The results in this paper provide valuable insights into the performance of frame synchronization for variable-length packets and can serve as a guideline for the deployment of future radio networks.

APPENDIX A

JUSTIFICATION OF EQUATION (4)

To simplify the analysis, we assume, without loss of generality, that attempts to perform frame synchronization continue indefinitely even after a correct marker acquisition. This assumption implies that M_i is well-defined for any $i \geq 1$.

To prove the claim, we begin by defining auxiliary random variables:

$$Y_i \triangleq \begin{cases} 1, & \text{if attempt } i \text{ yields a correct acquisition;} \\ 0, & \text{otherwise,} \end{cases}$$

for $i \geq 1$, and

$$I_{\mathcal{E}} \triangleq \begin{cases} 1, & \text{if event } \mathcal{E} \text{ occurs;} \\ 0, & \text{otherwise.} \end{cases} \quad (25)$$

Hence,

$$K = \inf\{i \geq 1 : Y_i = 1\}. \quad (26)$$

Let $S_K \triangleq M = M_1 + M_2 + \dots + M_K$. Then, similar to the proof of Wald's identity,

²²Note that changing the value of α will affect the asymptotic value.

²³This approach, however, can cause problems in some cases [55].

²⁴It is more convenient to obtain $\mathbb{E}\{M\}$ through the closed-form expression in (5) although $\mathbb{E}\{M\}$ can also be obtained from the pmf.

$$\begin{aligned} \mathbb{E}\{S_K\} &\stackrel{(a)}{=} \sum_{k=1}^{\infty} \mathbb{E}\{S_K I_{\{K=k\}}\} \\ &\stackrel{(b)}{=} \sum_{k=1}^{\infty} \sum_{i=1}^k \mathbb{E}\{M_i I_{\{K=k\}}\} \\ &\stackrel{(c)}{=} \sum_{i=1}^{\infty} \sum_{k=i}^{\infty} \mathbb{E}\{M_i I_{\{K=k\}}\} \\ &= \sum_{i=1}^{\infty} \mathbb{E}\{M_i I_{\{K \geq i\}}\}, \end{aligned} \quad (27)$$

where (a) is a summation over disjoint regions, (b) is due to the definition of S_k and linearity of expectation, and (c) is due to [56, Corr. to Thm. 1.27]. To show that M_i and $I_{\{K \geq i\}}$ are independent for any i , we write

$$\begin{aligned} I_{\{K \geq i\}} &= 1 - I_{\{K \leq i-1\}} \\ &= 1 - I_{\{Y_1=1 \text{ or } Y_2=1 \text{ or } \dots \text{ or } Y_{i-1}=1\}} \quad (\text{from eq. (26)}) \end{aligned}$$

which shows that $I_{\{K \geq i\}}$ is a function of $\mathbf{Y} \triangleq (Y_1, Y_2, \dots, Y_{i-1})$. Random vector \mathbf{Y} is independent of M_i because different acquisition attempts examine disjoint MSSs.²⁵ A continuation of (27) gives

$$\begin{aligned} \mathbb{E}\{S_K\} &= \sum_{i=1}^{\infty} \mathbb{E}\{M_i\} \mathbb{E}\{I_{\{K \geq i\}}\} \quad (\text{independence}) \\ &= \sum_{i=1}^{\infty} \mathbb{E}\{M_1\} \mathbb{P}\{K \geq i\} \quad (\text{identically distributed}) \\ &= \mathbb{E}\{M_1\} \mathbb{E}\{K\}, \end{aligned}$$

which proves the claim.²⁶

APPENDIX B

PROBABILITY OF CORRECT ACQUISITION

The probability of correct acquisition is given by

$$\begin{aligned} p_{\text{cAcq}} &= \mathbb{P}\left\{\bigcup_{i=1}^{\infty} \{V_1 : J_{i-1} \in \mathcal{R}^c, V_{J_i} \in \mathcal{R}\}\right\} \\ &= \sum_{i=1}^{\infty} \mathbb{P}\{V_1 : J_{i-1} \in \mathcal{R}^c, V_{J_i} \in \mathcal{R}\} \quad (\text{disjoint union}) \\ &= \underbrace{\mathbb{P}\{V_1 : J_1 \in \mathcal{R}^c, V_{J_1} \in \mathcal{R}\}}_{=p_{\text{det}}} \\ &\quad + \underbrace{\mathbb{P}\{V_1 : J_2 \in \mathcal{R}^c, V_{J_2} \in \mathcal{R}\}}_{=p_{\text{nal-det}}} \\ &\quad + \sum_{i=3}^{\infty} \mathbb{P}\{V_1 : J_{i-1} \in \mathcal{R}^c, V_{J_i} \in \mathcal{R}\}. \end{aligned}$$

²⁵In other words, \mathbf{Y} and M_i are independent because past decisions, which occurred at discrete times 1 to $i-1$, do not affect the future outcome at time i .

²⁶Note that the claim is not a direct application of Wald's identity [57, p. 369] because we do not require K to be a stopping time, do not require $\mathbb{E}\{K\} < \infty$, and do not require $\mathbb{E}\{M_i\} < \infty$.

Terms in the infinite sum can be simplified into

$$\begin{aligned}
& \mathbb{P}\{V_1:J_{i-1} \in \mathcal{R}^c, V_{J_i} \in \mathcal{R}\} \\
&= \underbrace{\mathbb{P}\{V_1:J_2 \in \mathcal{R}^c\}}_{=p_{\text{nal-nal}}} \\
&\times \left[\prod_{k=2}^{i-2} \mathbb{P}\{V_{J_k+1}:J_{k+1} \in \mathcal{R}^c \mid V_{J_k-\ell_{\text{max}}^m+2}:J_k \in \mathcal{R}^c\} \right] \\
&\times \mathbb{P}\{V_{J_{i-1}+1}:J_{i-1} \in \mathcal{R}^c, V_{J_i} \in \mathcal{R} \mid \\
&\quad V_{J_{i-1}-\ell_{\text{max}}^m+2}:J_{i-1} \in \mathcal{R}^c\} \\
&= p_{\text{nal-nal}}(c_{\text{nal}})^{i-3} c_{\text{det}} \quad (\text{Time invariance}),
\end{aligned}$$

where $\prod_{k=2}^1(\cdot) \triangleq 1$, $(c_{\text{nal}})^0 \triangleq 1$, and the parameters c_{nal} and c_{det} are defined in (6). Hence,

$$p_{\text{cAcq}} = p_{\text{det}} + p_{\text{nal-det}} + \sum_{i=3}^{\infty} p_{\text{nal-nal}}(c_{\text{nal}})^{i-3} c_{\text{det}}.$$

If $c_{\text{nal}} = 1$, then $c_{\text{det}} = 0$ and $p_{\text{cAcq}} = p_{\text{det}} + p_{\text{nal-det}}$. Otherwise, the infinite sum is a geometric series. Putting both cases of c_{nal} together yields (7).

APPENDIX C

EXPECTED TIME TO ACQUIRE A MARKER

The expected time to acquire a marker equals

$$\begin{aligned}
\mathbb{E}\{M_1\} &= \sum_{i=1}^{\infty} \mathbb{P}\{M_1 \geq i\} \\
&= 1 + \sum_{i=2}^{\infty} \mathbb{P}\{M_1 \geq i\},
\end{aligned}$$

since $M_1 \geq 1$. The probability in the infinite sum can be obtained by observing that $\{M_1 \geq i\} = \{V_1:J_{i-1} \in \mathcal{R}^c\}$. Hence,

$$\begin{aligned}
\mathbb{P}\{M_1 \geq 2\} &= \mathbb{P}\{V_1:J_1 \in \mathcal{R}^c\} = p_{\text{nal}} \\
\mathbb{P}\{M_1 \geq 3\} &= \mathbb{P}\{V_1:J_2 \in \mathcal{R}^c\} = p_{\text{nal-nal}},
\end{aligned}$$

and for $i \geq 4$,

$$\begin{aligned}
& \mathbb{P}\{M_1 \geq i\} \\
&= \mathbb{P}\{V_1:J_2 \in \mathcal{R}^c\} \\
&\times \prod_{k=2}^{i-2} \mathbb{P}\{V_{J_k+1}:J_{k+1} \in \mathcal{R}^c \mid V_{J_k-\ell_{\text{max}}^m+2}:J_k \in \mathcal{R}^c\} \\
&= p_{\text{nal-nal}}(c_{\text{nal}})^{i-3} \quad (\text{Time invariance}).
\end{aligned}$$

Hence

$$\mathbb{E}\{M_1\} = 1 + p_{\text{nal}} + p_{\text{nal-nal}} + \sum_{i=4}^{\infty} p_{\text{nal-nal}}(c_{\text{nal}})^{i-3}.$$

which simplifies into (8).

The expression for $\mathbb{E}\{M_1\}$, which involves three cases, can be understood intuitively as follows. The condition $0 < p_{\text{nal-nal}} \leq 1$ means that with non-zero probability a marker detector examines more than two MSSs. The condition $c_{\text{nal}} = 1$ implies that if the marker detector examines more than two MSSs, then the marker detector will never terminate. The condition $0 < p_{\text{nal-nal}} \leq 1$ together with $c_{\text{nal}} = 1$ in the third case implies that M_1 is unbounded, resulting in $\mathbb{E}\{M_1\} = \infty$.

The condition $p_{\text{nal-nal}} = 0$ in the second case implies that with probability one the marker detector terminates within one MSS or two MSSs, resulting in the expected duration $\mathbb{E}\{M_1\}$ between 1 and 2 inclusively. The remaining case occurs when the detector terminates after examining a finite number of MSSs, resulting in $1 \leq \mathbb{E}\{M\} < \infty$.

APPENDIX D

JUSTIFICATION OF (9)

The base case (9a) is obvious. The recursive case (9b) proceeds as follows:

$$\begin{aligned}
& \gamma(k+1, m) \\
&= \sum_{n=1}^{\infty} \mathbb{P}\{M_1 + M_2 + \dots + M_k + M_{k+1} \leq m \mid \\
&\quad M_{k+1} = n\} \mathbb{P}\{M_{k+1} = n\} \\
&= \sum_{n=1}^{\infty} \mathbb{P}\{M_1 + M_2 + \dots + M_k \leq m - n\} \mathbb{P}\{M_{k+1} = n\} \\
&\quad \sum_{n=1}^{m-k} \gamma(k, m-n) \mathbb{P}\{M_1 = n\},
\end{aligned}$$

where we have used the fact $M_1 + M_2 + \dots + M_k \geq k$ in the last equation.

APPENDIX E

JUSTIFICATION OF (10)

We will investigate properties of a generic arrival process, which include the marker arrival process $\{J_i\}$ as a special case. Then we will justify (10) through the properties of this generic arrival process.

Consider an arbitrary arrival process with the interarrival times $\{L_i + S_i\}$ for $i \geq 1$, where $L_i \geq 0$, $S_i \geq 1$, $\{L_i\}$ are i.i.d., $\{S_i\}$ are i.i.d., and $\{L_i\}$ and $\{S_i\}$ are independent. As an example, L_i is the length of a frame, and S_i is the length of a silent transmission plus the length of the marker. Suppose that we begin to observe the arrival process at random time. Let $L_{i^*} + S_{i^*}$ be the interarrival time containing the beginning of the observation. We wish to obtain the pmf of L_{i^*} .

We use an argument based on renewal theory to write, for $\ell \geq 0$,

$$\mathbb{P}\{L_{i^*} = \ell\} = \lim_{n \rightarrow \infty} \frac{\sum_{\substack{1 \leq i \leq n \\ L_i = \ell}} (L_i + S_i)}{\sum_{i=1}^n (L_i + S_i)} \quad \text{almost surely,}$$

where the argument of the limit is the portion of time that gives rise to the event $\{L_{i^*} = \ell\}$. Separating the summation in the numerator and introducing an auxiliary random set,

$$\mathcal{I}(\ell, n) \triangleq \{i : 1 \leq i \leq n \text{ and } L_i = \ell\},$$

into the expression give, almost surely,

$$\begin{aligned}
\mathbb{P}\{L_{i^*} = \ell\} &= \lim_{n \rightarrow \infty} \left(\frac{\ell |\mathcal{I}(\ell, n)| + \sum_{i \in \mathcal{I}(\ell, n)} S_i}{\sum_{i=1}^n (L_i + S_i)} \right) \\
&= \lim_{n \rightarrow \infty} \left(\frac{\frac{\ell |\mathcal{I}(\ell, n)|}{n} + \frac{|\mathcal{I}(\ell, n)| \sum_{i \in \mathcal{I}(\ell, n)} S_i}{n |\mathcal{I}(\ell, n)|}}{\frac{1}{n} \sum_{i=1}^n (L_i + S_i)} \right),
\end{aligned}$$

which simplifies into the expression at the bottom of the page. Writing

$$\frac{|\mathcal{I}(\ell, n)|}{n} = \frac{1}{n} \sum_{i=1}^n I_{\{L_i=\ell\}},$$

where I is the indicator function, defined in (25), and applying the strong law of large number [57, Thm. 8.3.5] to the limits result in

$$\mathbb{P}\{L_{i^*} = \ell\} = \frac{\ell \mathbb{P}\{L_1 = \ell\} + \mathbb{P}\{L_1 = \ell\} \mathbb{E}\{S_1\}}{\mathbb{E}\{L_1 + S_1\}},$$

or equivalently,

$$\mathbb{P}\{L_{i^*} = \ell\} = \left(\frac{\ell + \mathbb{E}\{S_1\}}{\mathbb{E}\{L_1\} + \mathbb{E}\{S_1\}} \right) \mathbb{P}\{L_1 = \ell\}. \quad (28)$$

We make the following observations regarding (28). If L_i takes values in a set \mathcal{L} of integers, then L_{i^*} also takes values in the same set of integers. This characteristic of L_{i^*} is expected, since L_{i^*} is one of $\{L_i : i \geq 1\}$. In addition, for all ℓ , the right-hand sides of (28) are non-negative and sum to 1. This characteristic implies that (28) is a valid pmf. Moreover, if $L_i = \ell_c$ and $S_i = s_c$ are constants, then (28) becomes

$$\mathbb{P}\{L_{i^*} = \ell\} = \begin{cases} 1, & \text{if } \ell = \ell_c; \\ 0, & \text{otherwise,} \end{cases}$$

which agrees with intuition. Furthermore, the expectation of L_{i^*} satisfies²⁷

$$\begin{aligned} \mathbb{E}\{L_{i^*}\} &= \frac{\mathbb{E}\{L_1^2\} + \mathbb{E}\{L_1\} \mathbb{E}\{S_1\}}{\mathbb{E}\{L_1\} + \mathbb{E}\{S_1\}} \\ &\geq \mathbb{E}\{L_1\}, \end{aligned}$$

indicating that L_{i^*} tends to be larger than L_1 . This characteristic is intuitive, since the random instant that our observation begins is likely to fall into a large interarrival time. These observations help to validate (28).

Using (28) with

$$L_i = L_i^d, S_i = L_i^s + \ell_{\max}^m, \ell = \ell_0^d, \text{ and } L_{i^*} = L_0^d$$

gives (10a). Similarly, using (28) with

$$L_i = L_i^s, S_i = L_i^d + \ell_{\max}^m, \ell = \ell_0^s, \text{ and } L_{i^*} = L_0^s$$

gives (10b).

APPENDIX F VALUE OF $\tilde{N}(k)$

We decompose

$$\tilde{N}(k) = \tilde{N}_{\text{nal}}(k) + \tilde{N}_{\text{det}}(k),$$

²⁷The inequality follows from the fact that variance $\mathbb{E}\{L^2\} - (\mathbb{E}\{L\})^2$ is non-negative for any random variable L , or more generally, from the Schwarz inequality [56, Thm. 3.5].

where $\tilde{N}_{\text{nal}}(k)$ denotes the number of k -joint probabilities required to evaluate the transition probabilities p_{nal} , $p_{\text{nal-nal}}$, and c_{nal} , and $\tilde{N}_{\text{det}}(k)$ denotes the number of k -joint probabilities required to evaluate the transition probabilities p_{det} , $p_{\text{nal-det}}$, and c_{det} . To obtain $\tilde{N}_{\text{nal}}(k)$, we consider six distinct cases.

Case 1a: $L_i^s = 0$ and $1 \leq k \leq \ell_{\max}^m - 2$. Then, $\tilde{N}_{\text{nal}}(k) = 1$, which corresponds to the k -joint probability term generated by the sequence of k data symbols and the marker.

Case 2a: $L_i^s \geq 2\ell_{\max}^m - 2$ and $1 \leq k \leq \ell_{\max}^m - 2$. Then, $\tilde{N}_{\text{nal}}(k) = k$, which corresponds to the k -joint probability terms generated by the sequences of d data symbols, $k-d-1$ silence symbols, and the marker, for $d = 0, 1, 2, \dots, k-1$.

Case 3a: $L_i^s = 0$ and $k = \ell_{\max}^m - 1$. By inspection of Fig. 7, $\tilde{N}_{\text{nal}}(\ell_{\max}^m - 1)$ is the number of $(\ell_{\max}^m - 1)$ -joint probability terms generated by the sequence of $c_3, c_4, \dots, c_{\ell_{\max}^m}$, $(2\ell_{\max}^m - 2)$ data symbols, the marker, and $(\ell_{\max}^m - 1)$ data symbols. Hence, $\tilde{N}_{\text{nal}}(\ell_{\max}^m - 1) = 3\ell_{\max}^m - 2$.

Case 4a: $L_i^s \geq 2\ell_{\max}^m - 2$ and $k = \ell_{\max}^m - 1$. By inspection of Fig. 7, $\tilde{N}_{\text{nal}}(\ell_{\max}^m - 1)$ is the number of $(\ell_{\max}^m - 1)$ -joint probability terms generated by the sequence of $c_3, c_4, \dots, c_{\ell_{\max}^m}$, $(2\ell_{\max}^m - 2)$ data symbols, $(2\ell_{\max}^m - 2)$ silence symbols, the marker, and $(\ell_{\max}^m - 1)$ data symbols. Hence, $\tilde{N}_{\text{nal}}(\ell_{\max}^m - 1) = 5\ell_{\max}^m - 4$.

Case 5a: $L_i^s = 0$ and $k = \ell_{\max}^m$. By inspection of Fig. 7, $\tilde{N}_{\text{nal}}(\ell_{\max}^m)$ is the number of ℓ_{\max}^m -joint probability terms generated by the sequence of $c_2, c_3, \dots, c_{\ell_{\max}^m}$, $(2\ell_{\max}^m - 1)$ data symbols, the marker, and $(\ell_{\max}^m - 1)$ data symbols. Hence, $\tilde{N}_{\text{nal}}(\ell_{\max}^m) = 3\ell_{\max}^m - 1$.

Case 6a: $L_i^s \geq 2\ell_{\max}^m - 2$ and $k = \ell_{\max}^m$. By inspection of Fig. 7, $\tilde{N}_{\text{nal}}(\ell_{\max}^m)$ is the number of ℓ_{\max}^m -joint probability terms generated by the sequence of $c_2, c_3, \dots, c_{\ell_{\max}^m}$, $(2\ell_{\max}^m - 1)$ data symbols, $(2\ell_{\max}^m - 1)$ silence symbols, the marker, and $(\ell_{\max}^m - 1)$ data symbols. Hence, $\tilde{N}_{\text{nal}}(\ell_{\max}^m) = 5\ell_{\max}^m - 2$.

After deriving p_{nal} , $p_{\text{nal-nal}}$, and c_{nal} , we already have most of the joint probability terms that are also required for the derivation of p_{det} , $p_{\text{nal-det}}$, and c_{det} . The remaining k -joint probability terms are the first terms of the right-hand side of (12) for $k = 1, 2, 3, \dots, \ell_{\max}^m - 2$. We now consider two distinct cases.

Case 1b: $L_i^s = 0$ and $1 \leq k \leq \ell_{\max}^m - 2$. Then, $\tilde{N}_{\text{det}}(k) = 1$, which corresponds to the k -joint probability term generated by the sequence of k data symbols and $c_1, c_2, \dots, c_{\ell_{\max}^m - 1}$.

Case 2b: $L_i^s \geq 2\ell_{\max}^m - 2$ and $1 \leq k \leq \ell_{\max}^m - 2$. Then, $\tilde{N}_{\text{det}}(k) = k + 1$, which corresponds to the k -joint probability terms generated by the sequences of d data symbols, $k-d$ silence symbols, and $c_1, c_2, \dots, c_{\ell_{\max}^m - 1}$, for $d = 0, 1, 2, \dots, k$.

Combining the results from cases 1a–6a and cases 1b–2b gives the bounds for $\tilde{N}(k)$ in (23).

ACKNOWLEDGMENTS

The authors wish to thank W. M. Gifford, U. J. Ferner, M. Levine, and S. Spilecki for their helpful suggestions and careful reading of the manuscript, K. Woradit for providing a

$$\frac{\ell \left(\lim_{n \rightarrow \infty} \frac{|\mathcal{I}(\ell, n)|}{n} \right) + \left(\lim_{n \rightarrow \infty} \frac{|\mathcal{I}(\ell, n)|}{n} \right) \left(\lim_{n \rightarrow \infty} \frac{\sum_{i \in \mathcal{I}(\ell, n)} S_i}{|\mathcal{I}(\ell, n)|} \right)}{\lim_{n \rightarrow \infty} \frac{1}{n} \sum_{i=1}^n (L_i + S_i)}$$

simulation program, and A. Genz for help with the numerical method described in [53].

REFERENCES

- [1] Federal Communications Commission, "Spectrum policy task force (Rep. ET Docket no. 02-135)," Nov. 2002.
- [2] P. Kolodzy *et al.*, "Next generation communications: Kickoff meeting," in *Proc. DARPA*, Oct. 2001.
- [3] M. McHenry, "Frequency agile spectrum access technologies," in *FCC Workshop Cogn. Radio*, May 2003.
- [4] G. Staple and K. Werbach, "The end of spectrum scarcity," *IEEE Spectr.*, vol. 41, no. 3, pp. 48–52, Mar. 2004.
- [5] S. Haykin, "Cognitive radio: Brain-empowered wireless communications," *IEEE J. Select. Areas Commun.*, vol. 23, no. 2, pp. 201–220, Feb. 2005.
- [6] R. Talluri, "Error-resilient video coding in the ISO MPEG-4 standard," *IEEE Commun. Mag.*, vol. 36, no. 6, June 1998.
- [7] M. Budagavi, W. R. Heinzelman, J. Webb, and R. Talluri, "Wireless MPEG-4 video communication on DSP chips," *IEEE Signal Processing Mag.*, Jan. 2000.
- [8] J. Hagenauer and T. Stockhammer, "Channel coding and transmission aspects for wireless multimedia," *Proc. IEEE*, vol. 87, no. 10, Oct. 1999.
- [9] M. G. Martini, M. Mazzotti, M. Chiani, G. Panza, C. Lamy-Bergot, J. Huusko, G. Jeney, G. Feher, and S. X. Ng, "Controlling joint optimization of wireless video transmission: the PHOENIX basic demonstration platform," in *Proc. of 14th IST Mobile & Wireless Communication Summit*, Dresden, Germany, June 2005.
- [10] R. A. Scholtz, "Frame synchronization techniques," *IEEE Trans. Commun.*, vol. COM-28, no. 8, pp. 1204–1213, Aug. 1980.
- [11] J. J. Stiffler, *Theory of Synchronous Communications*, 1st ed. Englewood Cliffs, New Jersey 07632: Prentice-Hall, 1971.
- [12] W. Suwansantisuk, M. Z. Win, and L. A. Shepp, "Properties of the mean acquisition time for wide-bandwidth signals in dense multipath channels," in *Proc. 3rd SPIE Int. Symp. on Fluctuation and Noise in Communication Systems*, vol. 5847, Austin, TX, May 2005, pp. 121–135.
- [13] W. Suwansantisuk and M. Z. Win, "On the asymptotic performance of multi-dwell signal acquisition in dense multipath channels," in *Proc. IEEE Int. Zurich Seminar on Commun.*, Zürich, SWITZERLAND, Feb. 2006, pp. 174–177.
- [14] —, "Rapid acquisition techniques for spread spectrum signals," in *Proc. IEEE Int. Symp. on Inform. Theory*, Seattle, WA, July 2006, pp. 947–951.
- [15] W. Suwansantisuk, M. Z. Win, and L. A. Shepp, "On the performance of wide-bandwidth signal acquisition in dense multipath channels," *IEEE Trans. Veh. Technol.*, vol. 54, no. 5, pp. 1584–1594, Sept. 2005, special section on *Ultra-Wideband Wireless Communications—A New Horizon*.
- [16] W. Suwansantisuk and M. Z. Win, "Multipath aided rapid acquisition: Optimal search strategies," *IEEE Trans. Inform. Theory*, vol. 52, no. 1, pp. 174–193, Jan. 2007.
- [17] A. Polydoros and C. L. Weber, "A unified approach to serial search spread-spectrum code acquisition - part I: General theory," *IEEE Trans. Commun.*, vol. COM-32, no. 5, pp. 542–549, May 1984.
- [18] M. D. Katz, J. H. Iinatti, and S. Glisic, "Two-dimensional code acquisition in environments with a spatially nonuniform distribution of interference: Algorithm and performance," *IEEE Trans. Wireless Commun.*, vol. 3, pp. 1–7, Jan. 2004.
- [19] S. Vijayakumaran and T. F. Wong, "On equal-gain combining for acquisition of time-hopping ultra-wideband signals," *IEEE Trans. Commun.*, vol. 54, pp. 479–490, Mar. 2006.
- [20] L.-L. Yang and L. Hanzo, "Serial acquisition performance of single-carrier and multicarrier DS-SS-CDMA over Nakagami- m fading channels," *IEEE Trans. Wireless Commun.*, vol. 1, pp. 692–702, Oct. 2002.
- [21] S. Gezici, E. Fishler, H. Kobayashi, H. V. Poor, and A. F. Molisch, "A rapid acquisition technique for impulse radio," in *Proc. IEEE Pacific Rim Conf. on Commun., Computers and Signal Processing*, vol. 2, Victoria, Canada, Aug. 2003, pp. 627 – 630.
- [22] R. R. Rick and L. B. Milstein, "Parallel acquisition in mobile DS-SS-CDMA systems," *IEEE Trans. Commun.*, vol. 45, pp. 1466–1476, Nov. 1997.
- [23] A. E. Payzin, "Analysis of a digital bit synchronizer," *IEEE Trans. Commun.*, vol. 31, no. 4, pp. 554–560, Apr. 1983.
- [24] C. N. Georghiadis, "Optimum delay and sequence estimation from incomplete data," *IEEE Trans. Inform. Theory*, vol. 36, no. 1, pp. 202–208, Jan. 1990.
- [25] C. N. Georghiadis and D. L. Snyder, "The expectation-maximization algorithm for symbol unsynchronized sequence detection," *IEEE Trans. Commun.*, vol. 39, no. 1, pp. 54–61, Jan. 1991.
- [26] H. Wymeersch and M. Moeneclaey, "Code-aided ML joint delay estimation and frame synchronization," in *Signal Processing for Telecommunications and Multimedia, Multimedia Systems and Applications*, B. H. T.A. Wysocki and B. Wysocky, Eds., vol. 27. Springer-Verlag, 2005.
- [27] F. Simoons, H. Wymeersch, H. Steendam, and M. Moeneclaey, "Synchronization for MIMO systems," in *Smart Antennas - State-of-the-Art*. Hindawi Publishing, 2005.
- [28] M. Guenach, H. Wymeersch, H. Steendam, and M. Moeneclaey, "Code-aided ML joint frame synchronization and channel estimation for downlink MC-CDMA," *IEEE J. Select. Areas Commun.*, vol. 24, no. 6, pp. 1105–1114, June 2006.
- [29] H. Wymeersch, H. Steendam, H. Bruneel, and M. Moeneclaey, "Code-aided frame synchronization and phase ambiguity resolution," *IEEE Trans. Signal Processing*, vol. 54, no. 7, pp. 2747–2757, July 2006.
- [30] Y. Wang, S. Wenger, J. Wen, and A. K. Katsaggelos, "Error-resilient video coding techniques," *IEEE Signal Processing Mag.*, vol. 17, p. 6182, Apr. 2000.
- [31] W. Fischer, E. Wallmeier, T. Worster, S. P. Davis, and A. Hayter, "Data communications using ATM: architectures, protocols, and resource management," *IEEE Commun. Mag.*, vol. 32, pp. 24–33, Aug. 1994.
- [32] G.-G. Bi, "Performance of frame sync acquisition algorithms on the awgn channel," *IEEE Trans. Commun.*, vol. 32, no. 10, pp. 1196–1201, Oct. 1983.
- [33] H. Huh and J. V. Krogmeier, "A unified approach to optimum frame synchronization," *IEEE Trans. Wireless Commun.*, vol. 5, no. 12, pp. 3700–3711, Dec. 2006.
- [34] J. L. Massey, "Optimal frame synchronization," *IEEE Trans. Commun.*, vol. COM-20, no. 2, pp. 115–119, Apr. 1972.
- [35] P. Robertson, "A generalized frame synchronizer," in *Proc. IEEE Global Telecomm. Conf.*, Orlando, FL, Dec. 1992, pp. 365–369.
- [36] M. Chiani and M. G. Martini, "Optimum synchronization of frames with unknown, variable lengths on gaussian channels," in *Proc. IEEE Global Telecomm. Conf.*, Dallas, TX, Dec. 2004, pp. 4087–4091.
- [37] —, "Practical frame synchronization for data with unknown distribution on AWGN channels," *IEEE Commun. Lett.*, vol. 9, no. 5, pp. 456–458, May 2005.
- [38] —, "On sequential frame synchronization in AWGN channels," *IEEE Trans. Commun.*, vol. 54, no. 2, pp. 339–348, Feb. 2006.
- [39] R. H. Barker, "Group synchronization of binary digital systems," in *Communication Theory*, W. Jackson, Ed. New York: Academic-Butterworth, 1953.
- [40] S. W. Golomb and R. A. Scholtz, "Generalized Barker sequences," *IEEE Trans. Inform. Theory*, vol. IT-11, no. 4, pp. 533–537, Oct. 1965.
- [41] S. W. Golomb and M. Z. Win, "Recent results on polyphase sequences," *IEEE Trans. Inform. Theory*, vol. 44, no. 2, pp. 817–824, Mar. 1998.
- [42] A. Steingass, A. J. van Wijngaarden, and W. Teich, "Frame synchronization using superimposed sequences," in *Proc. IEEE Int. Symp. on Inform. Theory*, Ulm, GERMANY, June 1997, p. 489.
- [43] A. J. van Wijngaarden and T. J. Willink, "Frame synchronization using distributed sequences," *IEEE Trans. Commun.*, vol. 48, pp. 2127 – 2138, Dec. 2000.
- [44] B. Yang, K. B. Letaief, R. S. Cheng, and Z. Cao, "Burst frame synchronization for OFDM transmission in multipath fading links," in *Proc. IEEE Semiannual Veh. Technol. Conf.*, Amsterdam, NETHERLAND, Sept. 1999, pp. 300–304.
- [45] C. W. Yak, Z. Lei, S. Chattong, and T. T. Tjhung, "Timing synchronization and frequency offset estimation for ultra-wideband (UWB) multi-band OFDM systems," in *Proc. IEEE Int. Symp. on Personal, Indoor and Mobile Radio Commun.*, Berlin, Germany, Sept. 2005, pp. 471–475.
- [46] M. K. Howlader, "Decoder-assisted noncoherent frame synchronization for burst OFDM-based packet transmission," in *Proc. IEEE Global Telecomm. Conf.*, St. Louis, MO, Nov. 2005, pp. 2927–2931.
- [47] L. D. Kabulepa, A. G. Ortiz, and M. Glesner, "Design of an efficient OFDM burst synchronization scheme," in *IEEE Int. Symp. on Circuits and Systems*, vol. 3, Scottsdale, AZ, May 2002, pp. III-449 – III-452.
- [48] D. P. Bertsekas and J. N. Tsitsiklis, *Introduction to Probability*. Belmont, MA: Athena Scientific, 2002.
- [49] W. H. Press, S. A. Teukolsky, W. T. Vetterling, and B. P. Flannery, *Numerical Recipes in C*, 2nd ed. New York, NY 10011-4211: Cambridge University Press, 1995.
- [50] I. S. Gradshteyn and I. M. Ryzhik, *Tables of Integrals, Series, and Products*, 6th ed. San Diego, CA: Academic Press, Inc., 2000.
- [51] P. J. Bickel and K. Doksum, *Mathematical Statistics: Basic Ideas and Selected Topics*, 2nd ed. Upper Saddle River, NJ: Prentice Hall, 2001, vol. 1.
- [52] J. G. Proakis, *Digital Communications*, 4th ed. New York, NY, 10020: McGraw-Hill, Inc., 2000.

- [53] A. Genz, "Numerical computation of multivariate normal probabilities," *J. Computational and Graphical Statistics*, vol. 1, no. 2, pp. 141–149, June 1992.
- [54] D. P. Bertsekas and R. G. Gallager, *Data Networks*, 2nd ed. New Jersey, 07632: Prentice-Hall, 1992.
- [55] D. Fiorini, M. Chiani, V. Tralli, and C. Salati, "Can we trust in HDLC?" *ACM SIGCOMM Computer Commun. Review*, vol. 24, no. 5, pp. 61–80, Oct. 1994.
- [56] W. Rudin, *Real and Complex Analysis*, 3rd ed. McGraw-Hill, 1987.
- [57] R. M. Dudley, *Real Analysis and Probability*, 2nd ed. New York, NY: Cambridge University Press, 2003.



Watcharapan Suwansantisuk (S'04) received the B.S. degrees (with Honors) in Electrical and Computer Engineering and in Computer Science from Carnegie Mellon University in 2002. He received the M.S. degree in Electrical Engineering from the Massachusetts Institute of Technology (MIT) in 2004.

Since 2002, Watcharapan Suwansantisuk has been with the Laboratory for Information and Decision Systems (LIDS) at MIT, where he is now a Ph.D. candidate. His main research interests are commu-

nication theory and synchronization theory with applications to ultra-wide bandwidth (UWB) systems. He spent the summer of 2005 at the Istituto di Elettronica e di Ingegneria dell'Informazione e delle Telecomunicazioni (IEIIT) of the University of Bologna in Italy as a visiting research scholar.

He served as a member of the Technical Program Committee (TPC) for the IEEE International Conference on Communications in 2007 and served as a member of the TPC for the IEEE Conference on Ultra Wideband in 2006. He received the Morris Joseph Levin Award in 2004 for best Master's thesis presentation from the Department of Electrical Engineering and Computer Science and a Claude E. Shannon Fellowship in 2007 at MIT. In 2006 he received a best paper award from the IEEE First International Conference on Next-Generation Wireless Systems (co-sponsored by IEEE Communications Society).



Marco Chiani (M'94-SM'02) was born in Rimini, Italy, in April 1964. He received the Dr. Ing. degree (*magna cum laude*) in Electronic Engineering and the Ph.D. degree in Electronic and Computer Science from the University of Bologna in 1989 and 1993, respectively. Dr. Chiani is a Full Professor at the II Engineering Faculty, University of Bologna, Italy, where he is the Chair in Telecommunication. During the summer of 2001 he was a Visiting Scientist at AT&T Research Laboratories in Middletown, NJ. He is a frequent visitor at the Massachusetts

Institute of Technology (MIT), where he presently holds a Research Affiliate appointment.

Dr. Chiani's research interests include wireless communication systems, MIMO systems, wireless multimedia, low density parity check codes (LD-PCC) and UWB. He is leading the research unit of CNIT/University of Bologna on Joint Source and Channel Coding for wireless video and is a consultant to the European Space Agency (*ESA-ESOC*) for the design and evaluation of error correcting codes based on LDPC for space CCSDS applications.

Dr. Chiani has chaired, organized sessions and served on the Technical Program Committees at several IEEE International Conferences. He was Co-Chair of the Wireless Communications Symposium at ICC 2004. In January 2006 he received the ICNEWS award "For Fundamental Contributions to the Theory and Practice of Wireless Communications." He is the past chair (2002-2004) of the *Radio Communications Committee* of the IEEE Communication Society and the current Editor of Wireless Communication for the *IEEE Transactions on Communications*.



Moe Z. Win (S'85-M'87-SM'97-F'04) received the B.S. degree (*magna cum laude*) from Texas A&M University, College Station, in 1987 and the M.S. degree from the University of Southern California (USC), Los Angeles, in 1989, both in Electrical Engineering. As a Presidential Fellow at USC, he received both an M.S. degree in Applied Mathematics and the Ph.D. degree in Electrical Engineering in 1998.

Dr. Win is an Associate Professor at the Laboratory for Information & Decision Systems (LIDS),

Massachusetts Institute of Technology (MIT). Prior to joining MIT, he spent five years at AT&T Research Laboratories and seven years at the Jet Propulsion Laboratory. His main research interests are the applications of mathematical and statistical theories to communication, detection, and estimation problems. Specific current research topics include measurement and modeling of time-varying channels, design and analysis of multiple antenna systems, ultra-wide bandwidth (UWB) systems, optical transmission systems, and space communications systems.

Professor Win has been actively involved in organizing and chairing a number of international conferences. He served as the Technical Program Chair for the IEEE Conference on Ultra Wideband in 2006, the IEEE Communication Theory Symposia of ICC-2004 and Globecom-2000, and the IEEE Conference on Ultra Wideband Systems and Technologies in 2002; Technical Program Vice-Chair for the IEEE International Conference on Communications in 2002; and the Tutorial Chair for the IEEE Semiannual International Vehicular Technology Conference in Fall 2001. He served as the chair (2004-2006) and secretary (2002-2004) for the *Radio Communications Committee* of the IEEE Communications Society. Dr. Win is currently an Editor for IEEE TRANSACTIONS ON WIRELESS COMMUNICATIONS. He served as Area Editor for *Modulation and Signal Design* (2003-2006), Editor for *Wideband Wireless and Diversity* (2003-2006), and Editor for *Equalization and Diversity* (1998-2003), all for the IEEE TRANSACTIONS ON COMMUNICATIONS. He was Guest-Editor for the 2002 IEEE JOURNAL ON SELECTED AREAS IN COMMUNICATIONS (Special Issue on Ultra-Wideband Radio in Multiaccess Wireless Communications).

Professor Win received the International Telecommunications Innovation Award from Korea Electronics Technology Institute in 2002, a Young Investigator Award from the Office of Naval Research in 2003, and the IEEE Antennas and Propagation Society Sergei A. Schelkunoff Transactions Prize Paper Award in 2003. In 2004, Dr. Win was named Young Aerospace Engineer of the Year by AIAA, and garnered the Fulbright Foundation Senior Scholar Lecturing and Research Fellowship, the Institute of Advanced Study Natural Sciences and Technology Fellowship, the Outstanding International Collaboration Award from the Industrial Technology Research Institute of Taiwan, and the Presidential Early Career Award for Scientists and Engineers from the United States White House. He was honored with the 2006 IEEE Eric E. Sumner Award "for pioneering contributions to ultra-wide band communications science and technology." Professor Win is an IEEE Distinguished Lecturer and elected Fellow of the IEEE, cited "for contributions to wideband wireless transmission."